LIGHT ELEMENT ANALYSIS
BY ELECTRON PROBE MICROANALYZER

A thesis submitted in partial fulfilment
of the requirements for
the degree of
Doctor of Philosophy

Shigeo TANUMA

The University of Tsukuba

1982

CONTENTS

Chapter 1. Introduction

The elements belonging to the second period in the periodic table, ie. boron, carbon, nitrogen, oxygen and fluorine, are called "light" elements, and are very important to study the characteristics of metals, heat-resistant materials, rocks and minerals. In many cases the diffusion and the segregation of these elements in micro area relate to the change of their properties, ie. retro-gradiation of heat-resistant materials, deterioration of metals, refractive indices of minerals etc. Therefore the light elements analysis in micro area is required.

Among those elements oxygen is especially important because the element is main component of rocks, minerals, and most inorganic compounds. However, there is no suitable method for analysis of oxygen in spite of the importance as stated above. Micro structures of natural rocks as well as synthetic ceramics are usually very complicated as mixture of various mineral phases. Therefore, the analysis of oxygen in micro area is also required.

On the other hand the electron probe microanalyzer can be applied to the analysis of the elements ($4 \leq Z$) in μm order area, and has been widely used for the investigation of segregation, oxidized surface layer and

to the analysis of inclusion in micro area. Quantitative analysis of light elements by this instrument, however, has neither been established nor fully investigated because the K_α lines of light elements affect absorption effect significantly.

The wavelength and energies of OK_α lines of light elements ($Z < 10$), which can be detected by electron probe microanalyzer, are given in Table 1-1. Most of these lines lie beyond the wavelength range of crystals ordinary used in Bragg spectrometers. However, large 2d spacing of soap film type pseudo-crystal, ie. lead stearate; 2d = 100 Å, lead lignocerate; 2d = 125 Å, enable the range to be extended to cover the wavelengths of K_α lines of light elements down to beryllium (Z=4) with K_α lines of 114 Å.

Assuming that the difficulties on measurements of light elements,ie. chemical shift and detection of X-rays, are overcome, and the measurements of accurate relative line intensity of the specimen and the standard are obtained, there remains the question of correction for matrix because the absorption effect for light element X-rays is especially serious since mass absorption coefficients for long wavelength X-ray are generally very large.

This thesis describes the absorption correction

Table 1-1 Characteristics of K_α lines of light elements

(after White and Jhonson, 1972)

Element	Z	Wavelength (Å)	Energy (eV)	Critical exitation energy (eV)
Be	4	114.0	109	112
B	5	67.6	183	192
C	6	44.7	277	284
N	7	31.6	392	400
O	8	23.6	525	532
F	9	18.3	677	687

for light element analysis for electron probe microanalyzer through the study of analysis of oxygen in several oxy-salts and oxides, ie. silicates, sulfates, double oxides etc.

Chapter 2 reports the comparison of ordinary used absorption corrections (simple Philibert, full Philibert and Yakowitz-Heinrich absorption correction) when applied to oxygen analysis in several silicates, sulfates, binary-oxides and double oxides of lanthanoid and niobium.

In chapter 3 new absorption corrections based on a Gaussian ionization distribution or normalized ionization distribution are proposed.

In chapter 4 these proposed corrections are compared with ordinary used correction equations using 160 microanalysis data of oxygen.

Chapter 5 reports the application of the new absorption correction to the determination of total oxygen, which includes the oxygen in water of crystallization and the oxygen in hydroxyl group. Results of total analysis of muscovite and zeolites using OK_{α} line are discussed. And the following fact is elucidated that the content of water and hydroxyl group in micro area of being analyzed could be determined by deducing the amount of oxygen which is in combination with metals

from the total amount of oxygen. Although the determination of the content of water and hydroxyl group in these samples in micro area have been a difficult problem on electron probe microanalysis, the content of them are decided by electron probe microanalyzer deducting the oxygen content combined with metals stoichiometrically from the total oxygen content.

Chapter 2. Determination of Oxygen by the Ordinary Used Absorption Corrections

1. Introduction

In the quantitative electron probe microanalysis of light elements a standard specimen having similar chemical composition to the sample has bee required. By the use of the standard specimen with the similar composition to the sample, the correction which have to be applied to convert measured data to quantitative results may be minimized, reducing the error caused by inaccurate correction models. Although this method may be regarded as satisfactory, is generally inconvenient because a large number of complex standard is required. And the standard of this kind is not always available with ease.

In this chapter the author carried out the oxygen analysis using aluminium oxide as a standard in order to decide the suitable measurement conditions and to establish the absorption correction for the practical analysis. The samples analyzed were several double oxides of lanthanoid and niobium, sulfates, silicates and binary oxides.

2. Deouble Oxides of Lanthanoid and Niobium

2.1 Experimental

2.1.1. System

The electron probe microanalyzer system used consists of a JEOL JXA-50A and a ACPS-XR control system, which is a special interface designed by ELIONIX.

2.1.2. Measurement Condition

Details of the measurement condition for oxygen analysis are shown in Table 2-1. As the line of OK_α is in the long wave-length region (23.6 Å), the line is excessively affected by the high order X-ray lines of other elements. In order to reduce the effect, the pulse height analyzer with the following details was used for descriminator : lower level 1.0 V, window 1.9 V and discriminator mode ; diff.

For the measurement of the intensity of OK_α the peak intensiry (P) was measured at the peak position of OK_α line for 20 sec. and the background intensiry (B) at the both side of OK_α line apart ± 1.75 Å from the peak position for 5 sec.. Then the net intensity was given as $L_{(cps)} = P_{(cps)} - B_{(cps)}$,
where $B = (B_+ + B_-)/2$.
The measurements were carried out 10 times on each

Table 2-1. Measurement conditions for oxygen analysis in double oxides of lanthanoid and niobium

X-ray take-off angle	: 35°
Accelerating voltage	: 5, 7, 10, 12, 15, 20 kV
Probe current	: 0.07 - 0.2 μA
Analyzing crystal	: Lead stearate

sample, and the average eliminated minimum and maximum value was used as the intensity of OK_α line.

2.1.3. Samples and Standard

The samples which were used for the examination of analytical condition and of absorption correction were Al_2O_3, ZrO_2, MgO and $LnNbO_4$ (Ln : La, Pr, Er, Tb, Gd). The $LnNbO_4$ samples were synthesized by Sugitani (1975), and the compositions were known. The standard for oxygen was used aluminium oxide.

Each sample was mounted together with the aluminium oxide standard in a same way. Smooth and flat surfaces were achieved by mechanical polishing on successively fine grades of abrassive down to 1μm diamond. The samples were made conducting by coating a thin layer of carbon.

2.2. Results and Discussion

2.2.1. Examination of Analytical Condition for Oxygen Analysis

As the accelerating voltege is very important for electron probe microanalysis, the P/B ratio versus accelerating voltage on OK_α measurement are shown in Fig. 2-1, and the line intensity of OK_α line versus accelerating voltage in Fig. 2-2. Fig. 2-1 shows that the P/B ratio curves have maxima, and as a result the

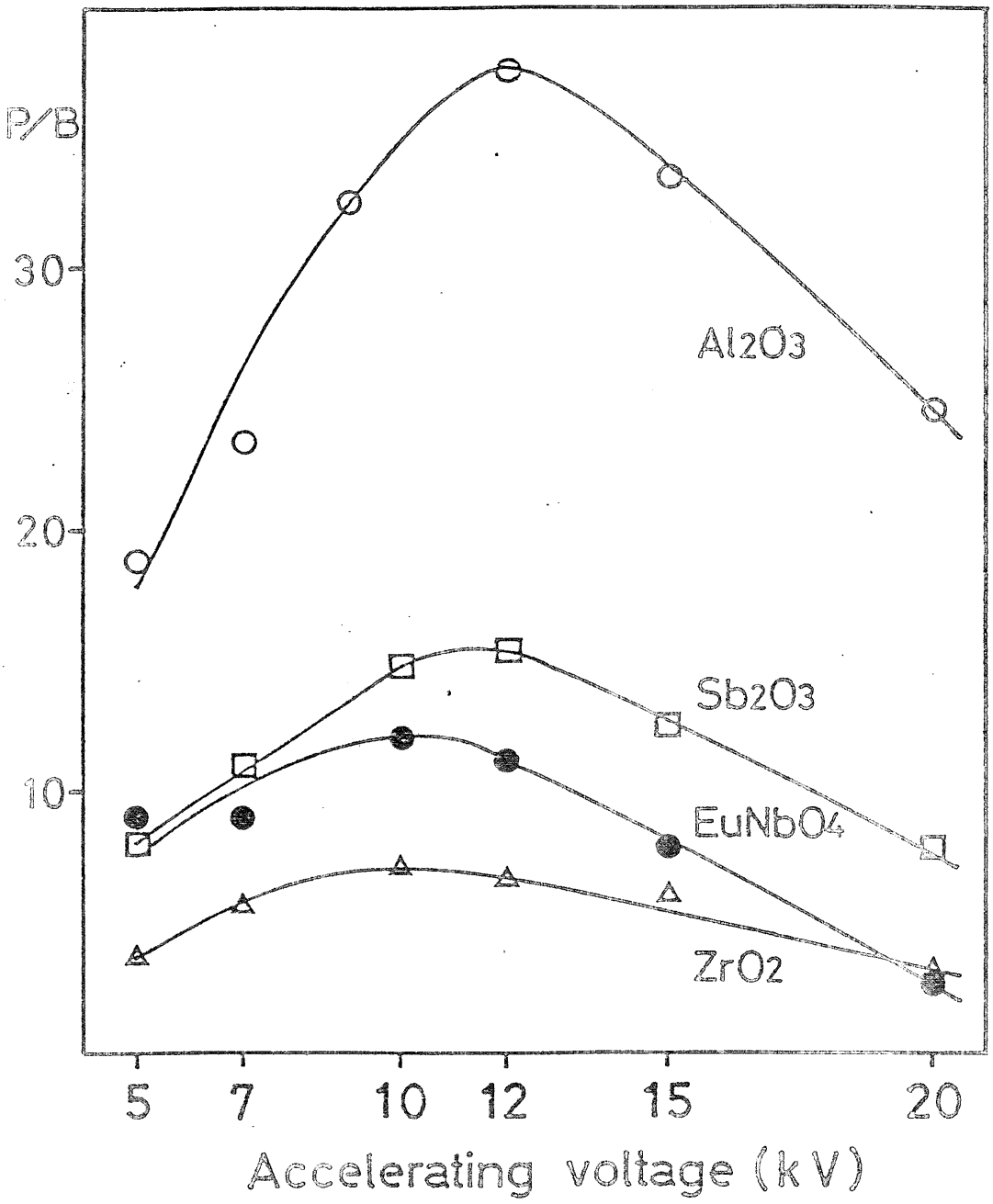

Fig. 2-1. P/B (P: peak intensity, B: background intensity) of OK_α line versus accelerating voltage for Al_2O_3, Sb_2O_3, $EuNbO_4$ and ZrO_2.

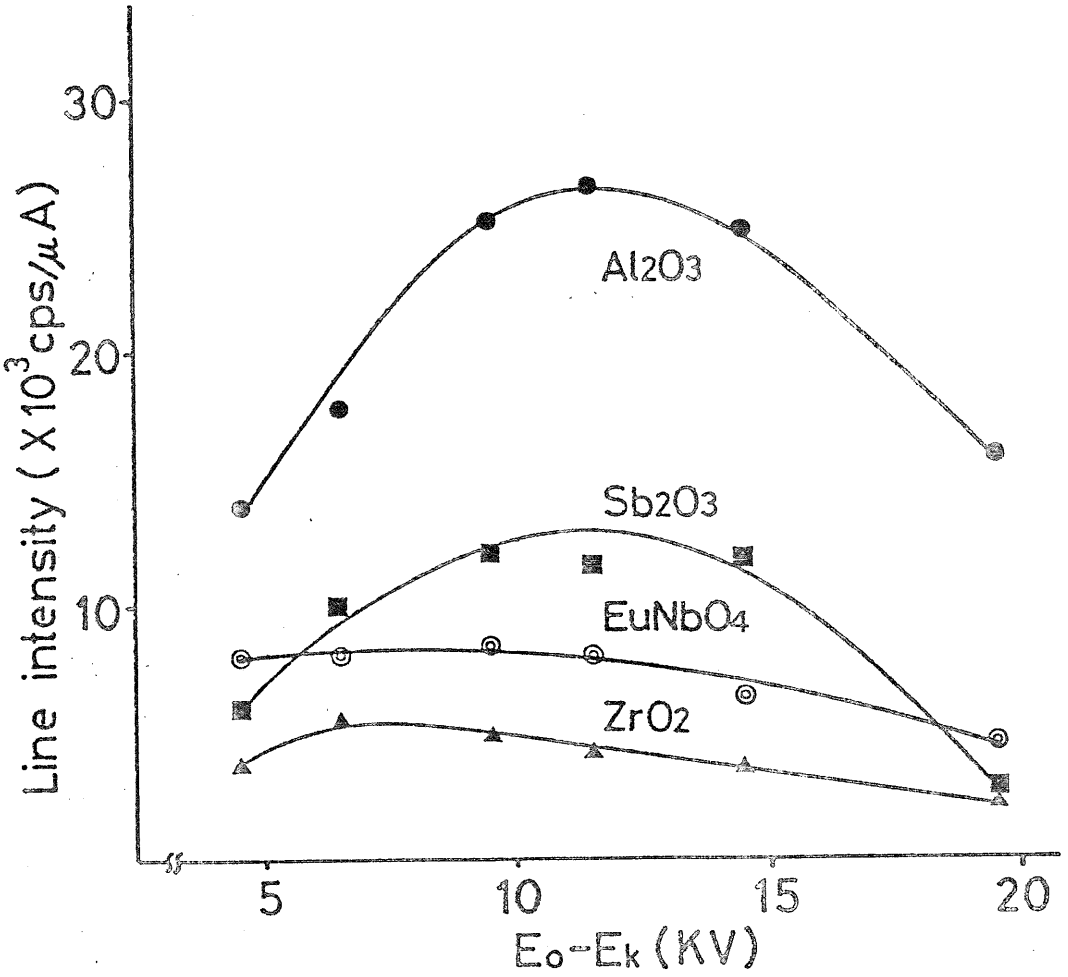

Fig. 2-2. Line intensity of OK_α line versus (E_0-E_k) (E_0: accelerating voltage, E_k: critical exitation energy) for Al_2O_3, Sb_2O_3, $EuNbO_4$ and ZrO_2.

suitable accelerating voltage is restricted to the region from 10 to 15 kV in practical analysis. Fig.2-2 shows that the line intensity curves of oxygen have maxima and are different from the results of ordinary element like iron in which the line intensity is roughly proportional to $(E_0 - E_c)^{1.67}$ (Green et al., 1961). The difference between them is due to the variation of ionization distribution and of absorption coefficient of these elements.

2.2.2. Examination of Ordinary Used Absorption Corrections

The generated X-ray is affected by the absorption effect and the line intensity emerged at an angle θ (X-ray take-off angle) to the surface may be written as

$$I = \int_0^\infty \phi(\rho z)\exp(-\chi\rho z)\,d(\rho z),$$

where $\chi=(\mu/\rho)\operatorname{cosec}\theta$, and μ/ρ is the mass absorption coefficient. As $f(\chi)$ represents the detected X-ray intensity, the above equation is written as

$$I = f(\chi) \int_0^\infty \phi(\rho z)\,d(\rho z)$$

$$\text{where } f(\chi) = \frac{\int_0^\infty \phi(\rho z)\exp(-\chi\rho z)\,d(\rho z)}{\int_0^\infty \phi(\rho z)\,d(\rho z)}$$

In the quantitative microanalysis, the theoretical X-ray intensity ratio of the sample to the standard is given as

$$k' = \frac{C \cdot f(\chi) \cdot \int_0^\infty \phi(\rho z)\,d(\rho z)}{C_{std} \cdot f(\chi)_{std} \cdot \int_0^\infty \phi(\rho z)_{std}\,d(\rho z)}$$

where the integral term $\int_0^\infty \phi(\rho z)\,d(\rho z) / \int_0^\infty \phi(\rho z)_{std}\,d(\rho z)$ is called "atomic number correction" and is usually calculated separatly from the absorption term. In this investigation the Duncumb-Reed atomic number correction (1968) was used and no fluorescence correction was applied because the X-ray fluoresence yield was very small compared with other factor in the light elements analysis. Mass absorption coefficients of OK_α were the values in the table given by Henke et al. (1974).

In the quantitative analysis of light elements by electron microprobe, absorption correction is the most important factor among the ZAF' correction (Z:Atomic number A :absorption, F:fluorescence correction),

and the following , three absorption corrections ; simple Philibert, full Philibert and Yakowitz -Heinrich correction, were examined.

i) simple Philibert correction (Love, et al. 1974b)

$$f(\chi) = (1+h)/(1+\chi/\sigma)/(1+h(1+\chi/\sigma))$$

where $h = 0.85, \Sigma C_i A_i / Z_i^2$, $\sigma = 6.8 \times 10^{-5}/(E_0^{1.86} - E_c^{1.86})$, E_0 : accelerating voltage, E_c : critical ionization energy, A : atomic weight and Z : atomic number.

ii) full Philibert correction (Love et al.,1974b)

$$f(\chi) = \frac{1 + \frac{\phi(0)h}{4 + \phi(0)h}\frac{\chi}{\sigma}}{(1 + \chi/\sigma)(1 + \frac{h}{1+h}\frac{\chi}{\sigma})}$$

where $\phi(0) = 1+2.8(1-0.9\ E_0/E_c)\cdot\eta$, $h = 1.5A/Z^2$ and

$$\sigma = 9.5 \times 10^5/(E_0^2 - E_c^2)$$

iii) Yakowitz-Heinrich correction (Heinrich, 1978)

$$f(\chi) = \{1+1.2 \times 10^{-6}(E_0^{1.65} - E_c^{1.65})\cdot\chi\}^{-2}$$

where $\chi = (\mu/\rho)$ cosec θ.

The observed X-ray intensiry ratios of OK_α using alminium oxide standard are shown in Table 2-2 as a function of accelerating voltage. In order to find the

Table 2-2. Measured X-ray intensity ratios of OK_α in double oxides of lanthanoid and niobium using aluminium oxide standard

Sample	Accelerating voltage (kV)					
	5	7	10	12	15	20
$LaNbO_4$	0.579	0.450	0.410	0.381	0.335	0.323
$PrNbO_4$	0.538	0.429	0.382	0.363	0.313	0.291
$EuNbO_4$	0.532	0.435	0.374	0.357	0.296	0.261
$GdNbO_4$	0.520	0.397	0.357	0.337	0.290	0.273
$TbNbO_4$	0.548	0.418	0.352	0.328	0.273	0.259

most suitable absorption correction the ratios k'/k are plotted in Figs. 2-3(simple Philibert correction), 2-4 (Yakowitz-Heinrich correction) and 2-5(full Philibert correction) as a function of accelerating voltage. Fig.2-5 shows the k' values predicted by the full Philibert correction are in close agreement with measured k values in the range $10 \leq E_0 \leq 20$ kV. The RMS errors of k'/k are shown in Table 2-3. This table shows the full Philibert correction gave satisfactory results for the practical analysis because of low RMS error (5%) in all measured accelerationg voltage region. On the other hand Yakowitz-Heinrich equation gave good results in the lower accelerating voltage region (Fig. 2-4). In high accelerating voltage region this equation cannot indicate correct value because the power on E_0 and E_c are inappropriate in the analysis of very light elements such as oxygen. On the other hand Fig.2-5 showed that the values predicted by the full Philibert equation agreed with the observed X-ray intensity ratios in high accelerating voltage region. This is due to the contribution of the $\phi(0)$ value for the correction in high accelerating voltage region. In the lower accelerating voltage range this equation does not give good results because the $\phi(0)$ value does not affect the correction in this reagion.

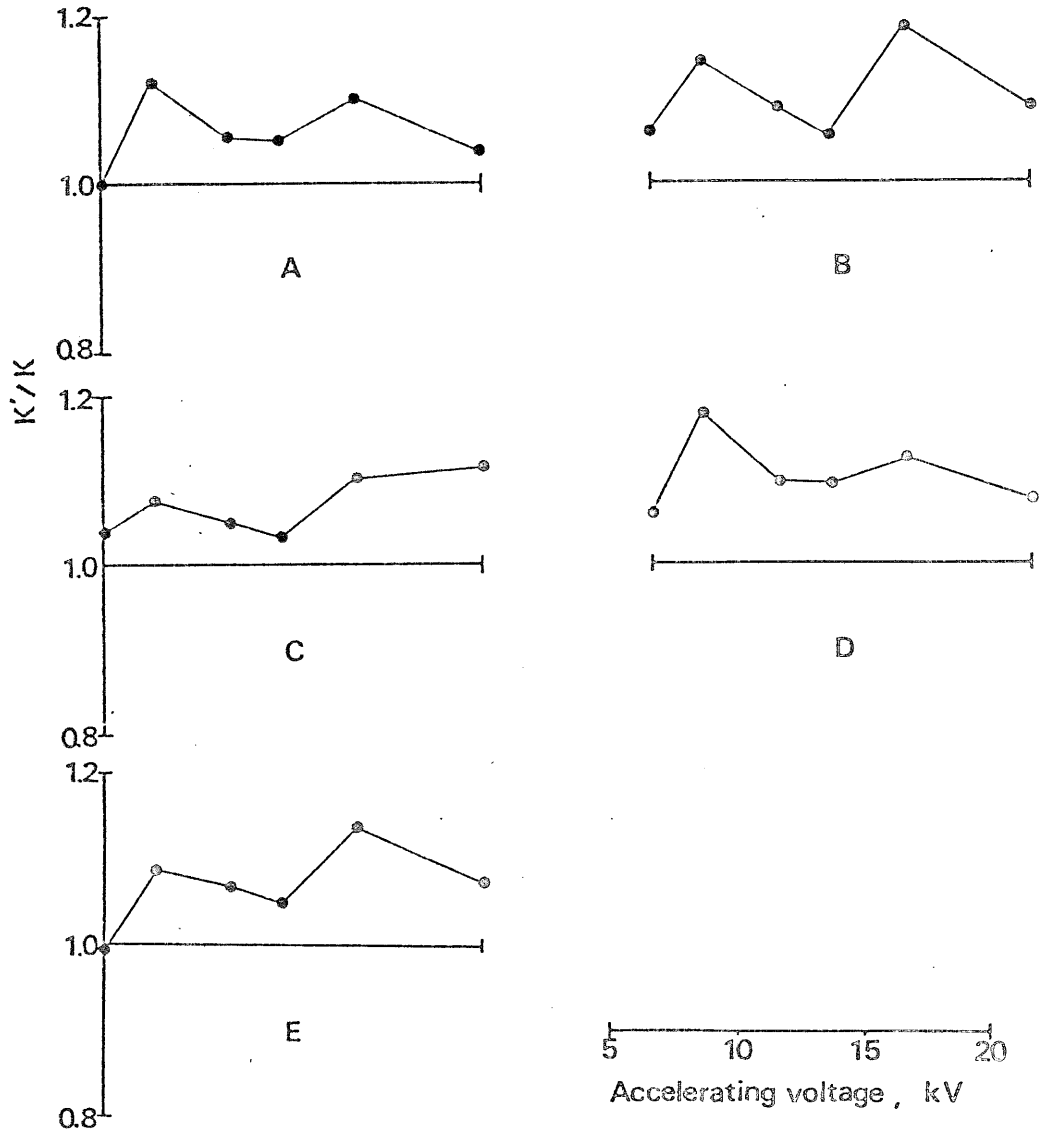

Fig. 2-3. Plots of k'/k using simple Philibert absorption correction together with Duncumb-Reed atomic number correction for $LaNbO_4$ (A), $EuNbO_4$ (B), $PrNbO_4$ (C), $GdNbO_4$ (D) and $TbNbO_4$ (E).

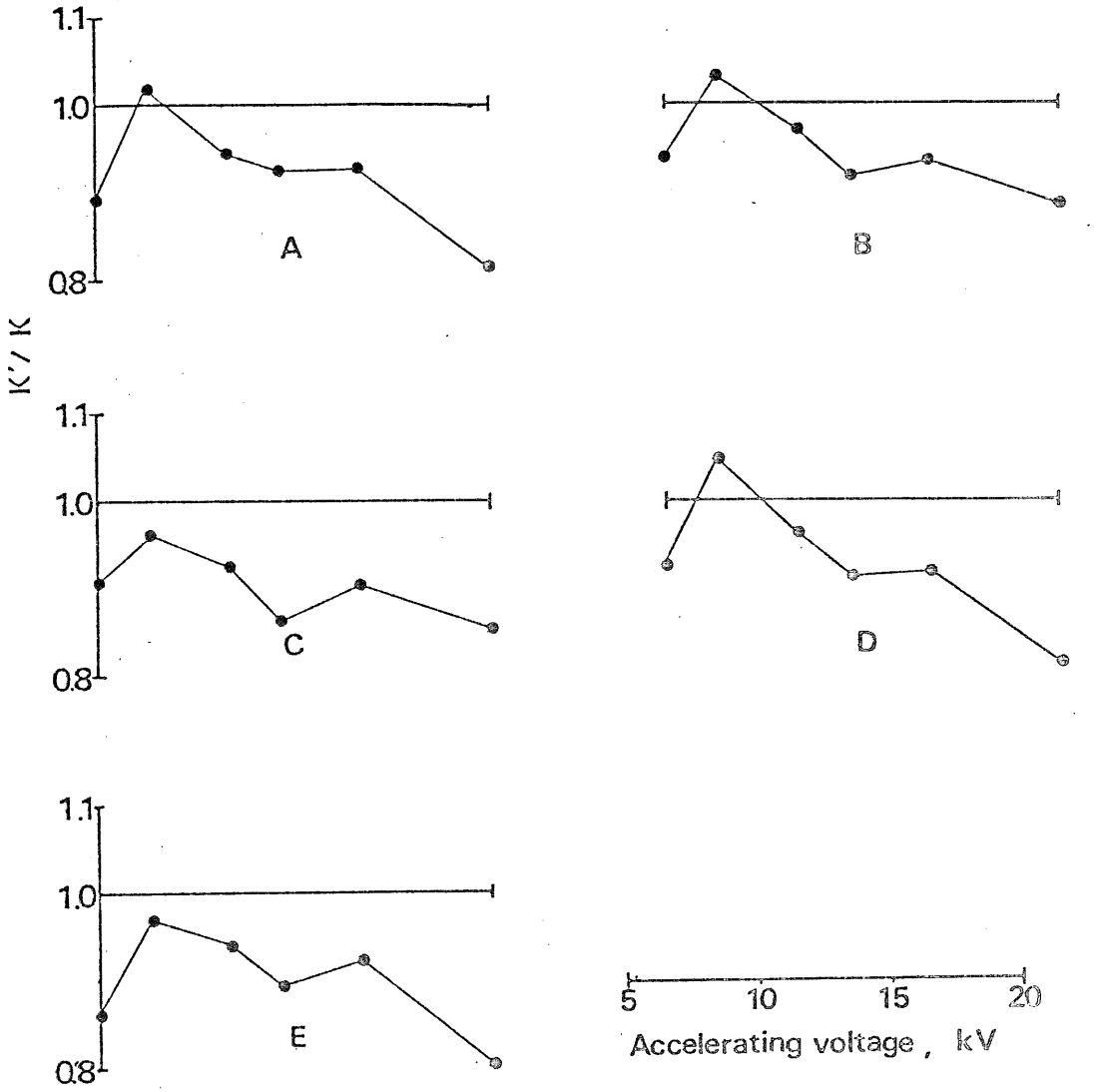

Fig. 2-4. Plots of k'/k using Yakowitz-Heinrich absorption correction together with Duncumb-Reed atomic number correction for $LaNbO_4$(A), $EuNbO_4$(B), $PrNbO_4$(C), $GdNbO_4$(D) and $TbNbO_4$(E).

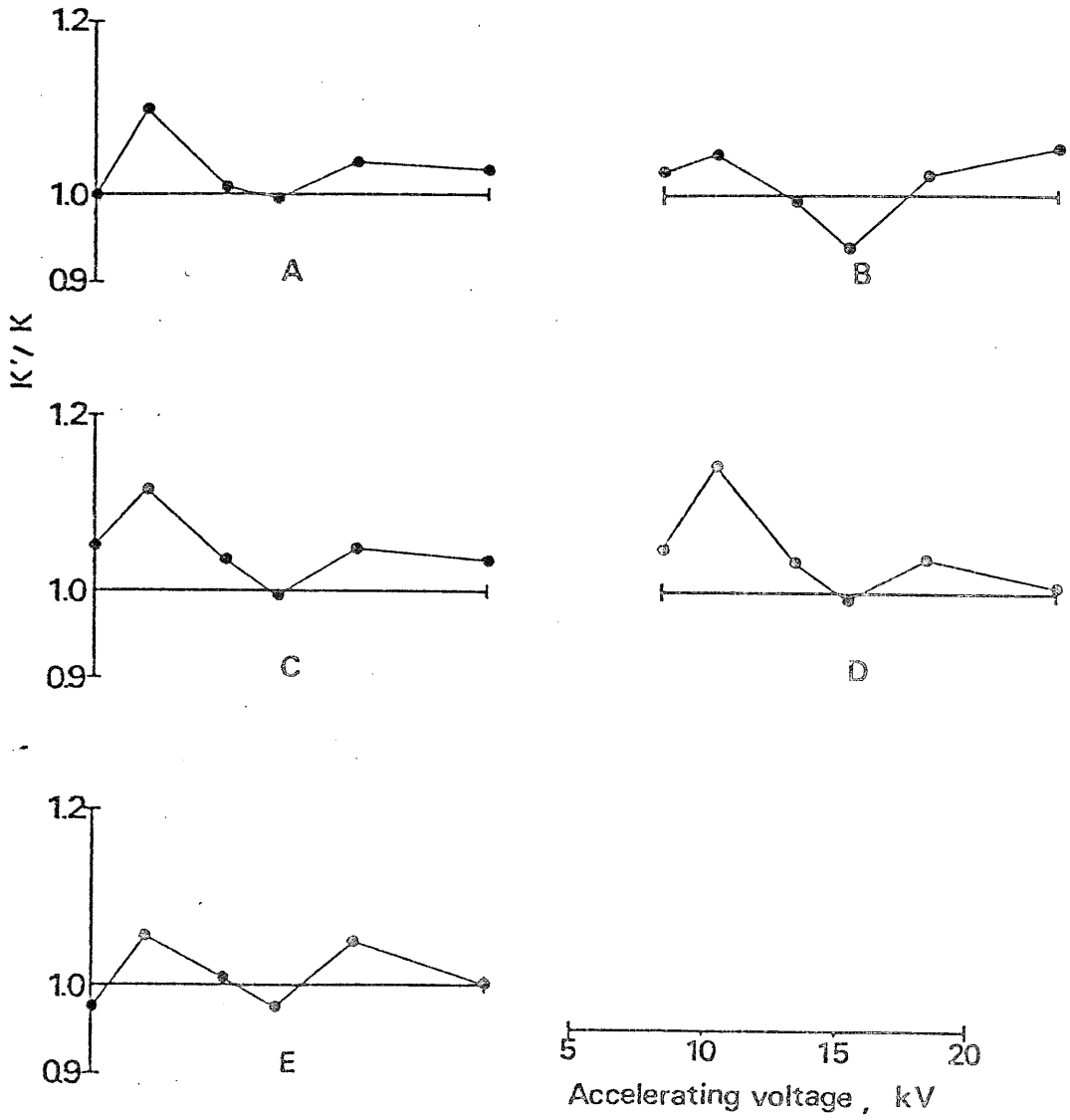

Fig. 2-5. Plots of k'/k using full Philibert absorption correction together with Duncumb-Reed atomic number correction for $LaNbO_4$(A), $EuNbO_4$(B), $PrNbO_4$(C), $GdNbO_4$(D) and $TbNbO_4$(E).

Table 2-3. RMS errors of oxygen analysis in double oxides of lanthanoid and niobium

Absorption correction	RMS error(%)* of k'/k
Simple Philibert	9.01
Full Philibert	5.02
Yakowitz-Heinrich	9.97

Atomic number correction : Duncumb-Reed equation

* Accelerating voltge : 5, 7, 10 , 12, 15 and 20 kV.

2.2.3. Results of analyses

Oxygen content of double oxides of lanthanoid and niobium were determined at accelerating voltage 10 and 12 kV, at which the P/B ratio curves gave maxima, and the full Philibert and the Duncumb-Reed atomic number correction were applied to the observed intensity ratios. Results of analyses are shown in Table 2-4. The accurate results of oxygen analysis (RMS error : 2.9%) at these accelerating voltage region indicate that those corrections are applicable to the practical analysis for oxygen in lanthanoid oxide compounds.

3. Sulfates

3.1. Experimental

Measurements of OK_{α} intensity of several sulfates were carried out at the accelerating voltage 5, 7, 10, 12, 15 and 20 kV. The details of the measuremtent conditions were similar to those described in the previous section 2. The standard used for oxygen was synthetic aluminium oxide. The analyzed samples were natural barite $BaSO_4$, celestite $SrSO_4$, anglesite $PbSO_4$ and anhydrite $CaSO_4$. The purity of these samples are sufficient enough for this investigation because the other elements than the main component were not detected by the qualitative microprobe analysis.

Table 2-4. Determination of oxygen content by full Philibert correction and Duncumb-Reed atomic number correction

Sample	Concentration (wt%)		
	10kV*	12kV*	Theoretical value**
$LaNbO_4$	21.4	21.7	21.6
$PrNbO_4$	20.7	21.6	21.5
$EuNbO_4$	20.8	22.0	20.7
$GdNbO_4$	19.7	20.5	20.4
$TbNbO_4$	20.0	20.7	20.3

* Accelerating voltage

** Calculated from ideal formula

3.2. Results and Discussion

3.2.1. Conditions for Measurement

The peak intensity P and the background intensity B were measured in the range $5 \leq E_0 \leq 20$ kV, and obtained P/B ratios for OK_α line versus accelerating voltge are plotted in Fig. 2-6. This figure indicates that the suitable accelerating voltage is in the range from 10 to 15 kV for the measurement of OK_α in sulfates.

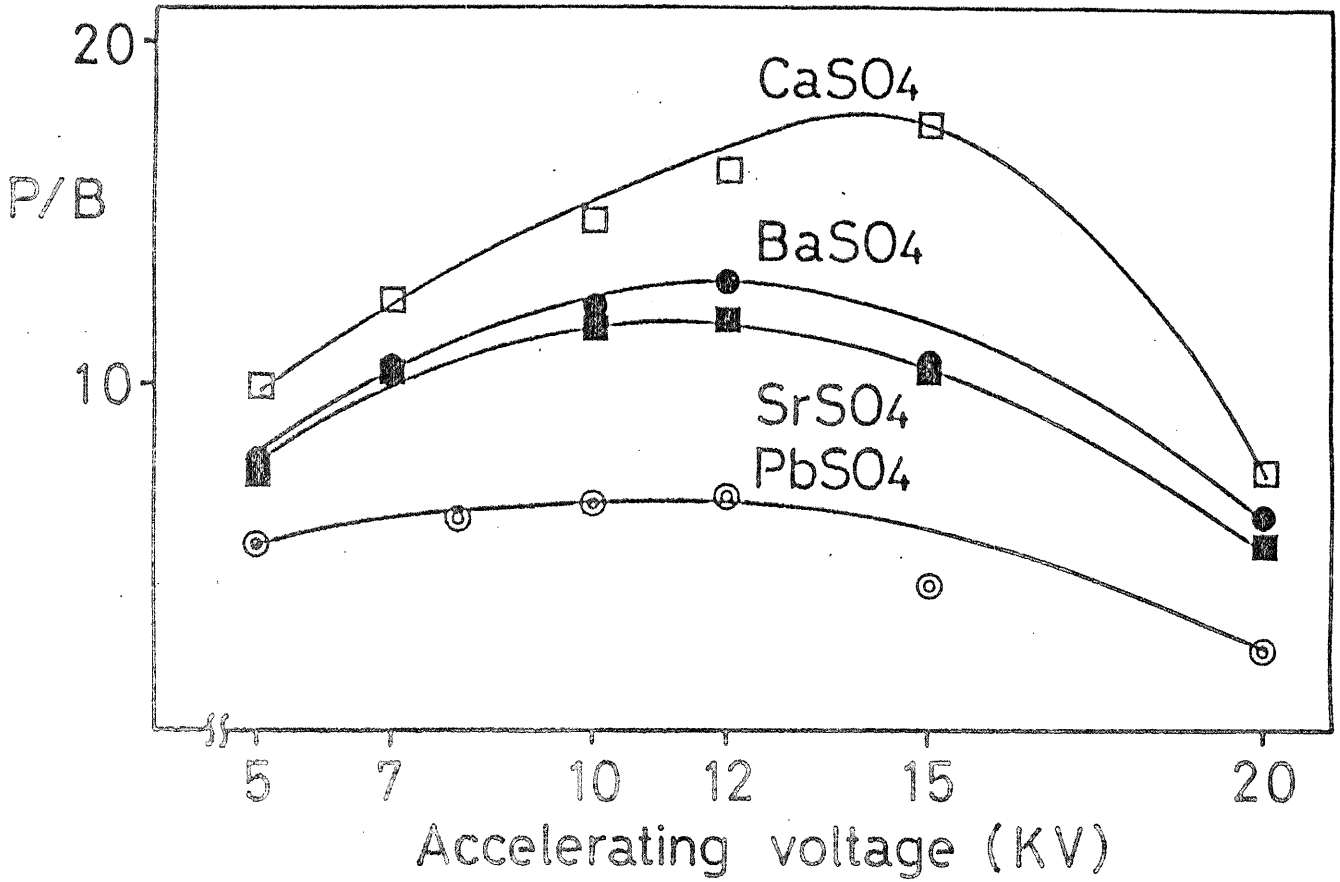

Fig. 2-6. P/B (P: peak intensity, B: background intensity) of OK_{α} line versus accelerating voltage for $CaSO_4$, $BaSO_4$, $SrSO_4$ and $PbSO_4$.

3.2.2. Examination of Absorption Correction

The observed X-ray intensity ratios using aluminium oxide standard are listed in Table 2-5 as a function of accelerating voltage. In order to find appropriate absorption correction for oxygen analysis in sulfates, the ratios k'/k (k :observed intensity ratio, k': theoretical intensity ratio calculated applying various absorption corrections together with Duncumb-Reed (1968) atomic number correction) are plotted in Figs.2-7 (simple Philibert), 8(full Philibert) and 9(Yakowitz-Heinrich) as a function of accelerating voltage. The RMS errors of k'/k for oxygen analysis are shown in Table 2-6. According to the results of Table 2-6 and these figures, no absorption correction was found which gave satisfactory agreement between the theoretical and observed X-ray intensiry ratios among all measured accelerating voltage range. The Yakowitz-Heinrich correction, gave somewhat better results at 5 and 7 kV as shown in Fig. 2-9. The calculated intensity ratios using this equation, however, did not agree with the observed X-ray intensity ratios in the range of high accelerating voltage, and this disagreement might be due to the contribution of the incorrect power in the term $E_0^{1.65} - E_c^{1.65}$. In the previous section on double oxides of lanthanoid and niobium, the full Philibert

Table 2-5 Measured X-ray intensity ratios of OK_α in sulfates using aluminium oxide standard

Sample	Accelerating voltage (kV)					
	5	7	10	12	15	20
$CaSO_4$	0.719	0.591	0.469	0.467	0.422	0.373
$SrSO_4$	0.664	0.547	0.434	0.407	0.392	0.354
$BaSO_4$	0.713	0.648	0.613	0.645	0.654	0.640
$PbSO_4$	0.415	0.330	0.264	0.266	0.211	0.201

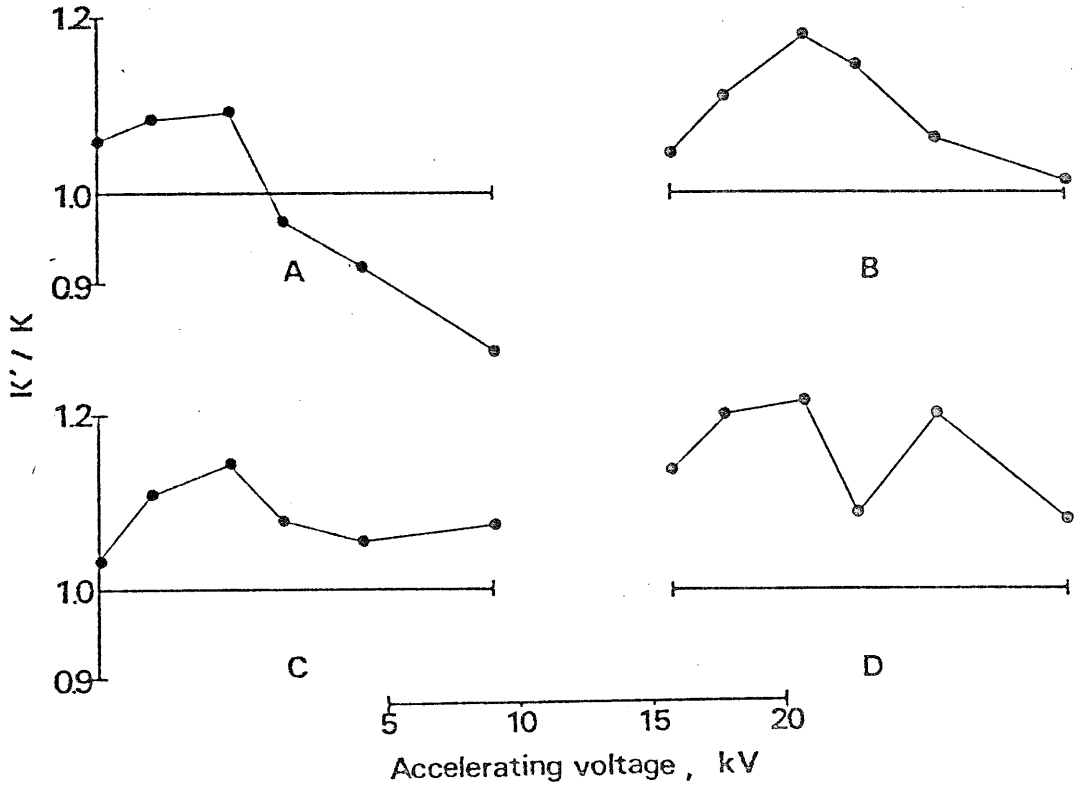

Fig. 2-7. Plots of k'/k using simple Philibert absorption correction together with Duncumb-Reed atomic number correction for $CaSO_4$(A), $SrSO_4$(B), $BaSO_4$(C) and $PbSO_4$.

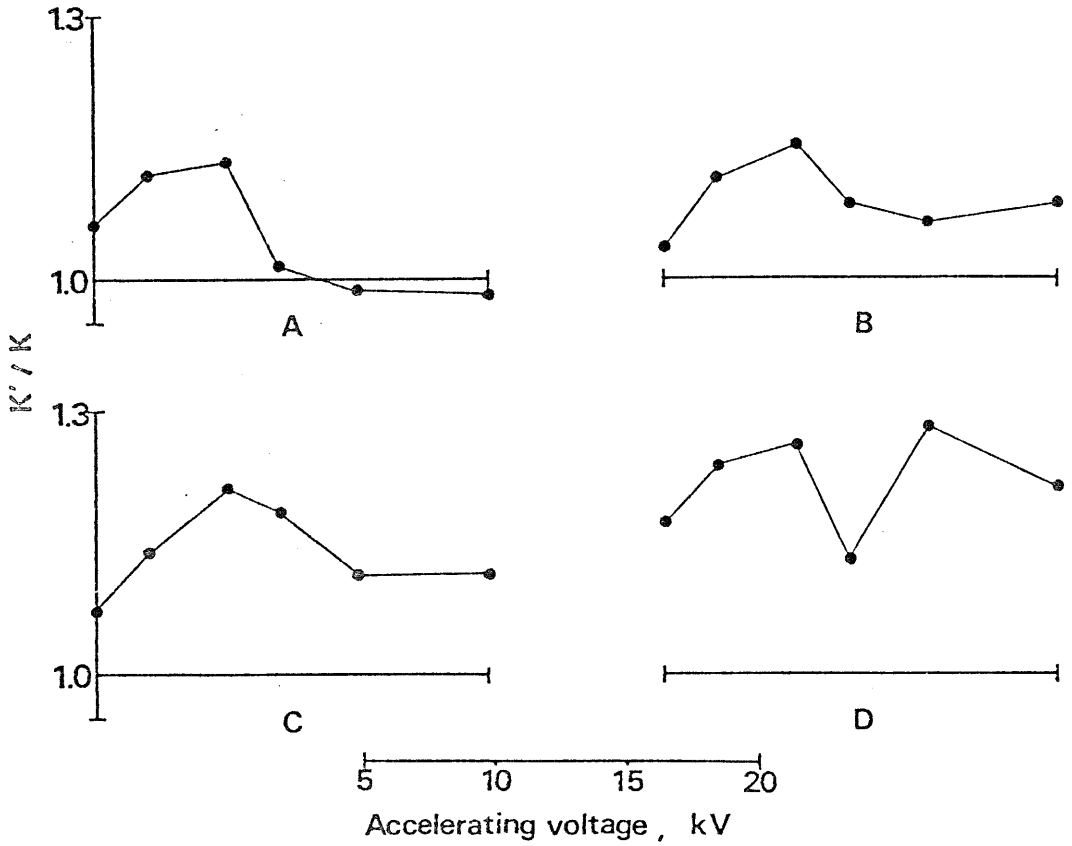

Fig. 2-8. Plots of k'/k using full Philibert absorption correction together with Duncumb-Reed atomic number correction for $CaSO_4$(A), $SrSO_4$(B), $BaSO_4$(C) and $PbSO_4$(D).

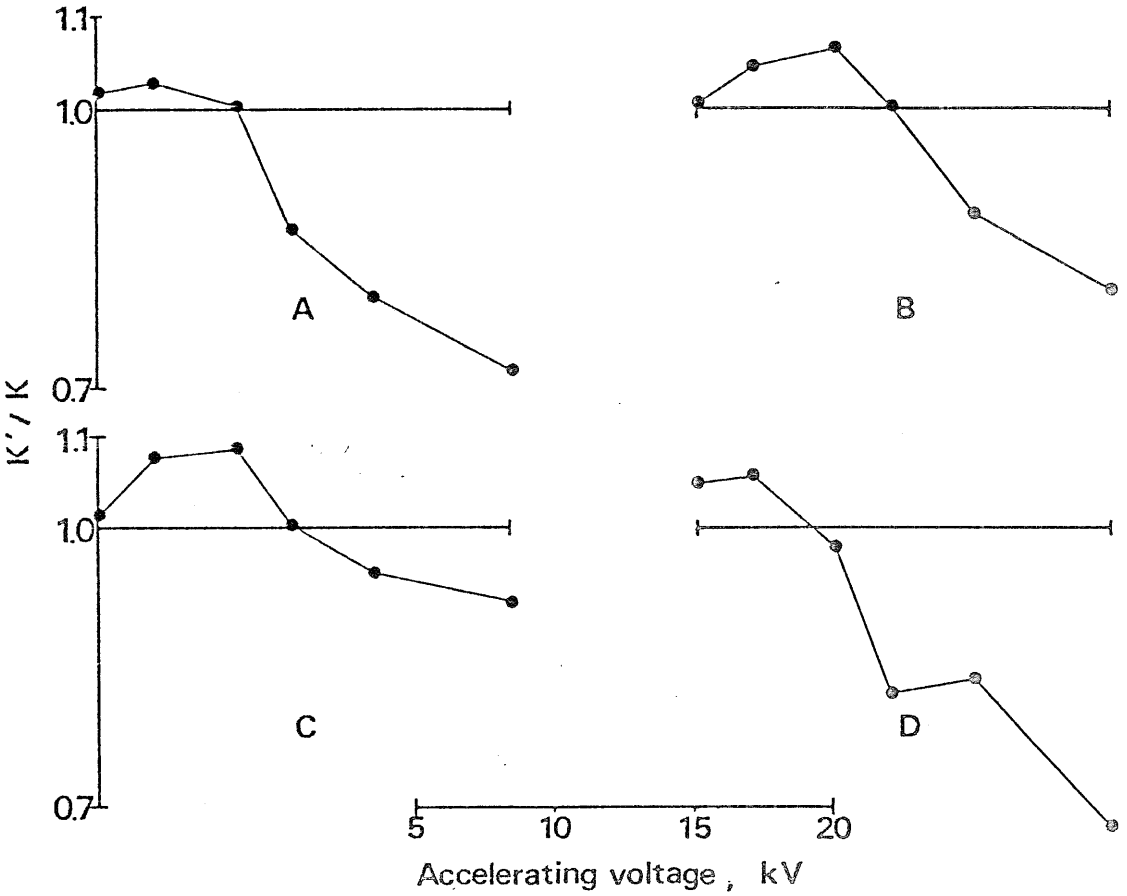

Fig. 2-9. Plots of k'/k using Yakowitz-Heinrich absorption correction together with Duncumb-Reed atomic number correction for $CaSO_4$(A), $SrSO_4$(B), $BaSO_4$(C) and $PbSO_4$(D).

Table 2-6. RMS errors of oxygen analysis in sulfates

Absorption correction	RMS error(%) of k'/k
Simple Philibert	11.8
Full Philibert	14.8
Yakowitze Heinrich	12.5

Atomic number correction : Duncumb-Reed equation

absorption correction gave good results in all measured accelerating voltage range, but this is not the case in this section. It seemed that the $\phi(0)$ value and ionization distribution model were not appropriate for oxygen analysis in sulfates.

On the other hand the Yakowitz-Heinrich and the simple Philibert absorption correction gave good results on sulfur analysis in sulfates. The RMS errors were 3.33% and 3.84% respectively in the range $12 \leq E_0 \leq 20$kV. Therefore there is no problem in the determination of sulfur for the practical analysis. The difference between the results of oxygen analysis and those of sulfur must be due to the variation of ionization distribution and absorption coefficients for each element.

4. Binary Oxides Systems

4.1. Experimental

Measurements of OK_α of several binary oxides were carried out at the accelerating voltage 10, 15, 20, 25 and 30 kV. The details of the measurement condition were similar to those described in the section 2. The analyzed samples were synthetic MgO, Cr_2O_3, TiO_2 and Fe_2O_3, and the standard for oxygen was synthetic aluminium oxide. The mass absorption coefficients of OK_α line were used the table given by Love et al. (1974b) (for the elements, $8 \leq Z < 22$) and that given by

Henke et al. (1974) (for the elements, $Z \geq 22$).

4.2. Results and Discussion

4.2.1. Examination of Analytical Condition

The P/B ratios observed on MgO, Cr_2O_3, TiO_2 and Fe_2O_3 versus accelerating voltage are shown in Fig. 2-10. This figure indicates the suitable accelerating voltage is in the range from 10 to 15 kV for measurement of OK_α in binary oxide systems.

4.2.2. Examination of Absorption Correction

The observed X-ray intensity ratios using alminium oxide standard are listed in Table 2-7 as a function of accelerating voltage. In this table the data of 5 kV and for MoO_3 and ZrO_2 are quoted from the results of Love et al. (1974b). The RMS errors of k'/k are shown in Table 2-8. The values for k'/k are plotted in Fig.2-11(simple Philibert), 2-12(full Philibert) and 2-13(Yakowitz-Heinrich) as a function of accelerating voltage. The table and these figures show that there is no absorption correction which gives satisfactory results even in the high P/B region. Therefore a new absorption correction is required for oxygen analysis.

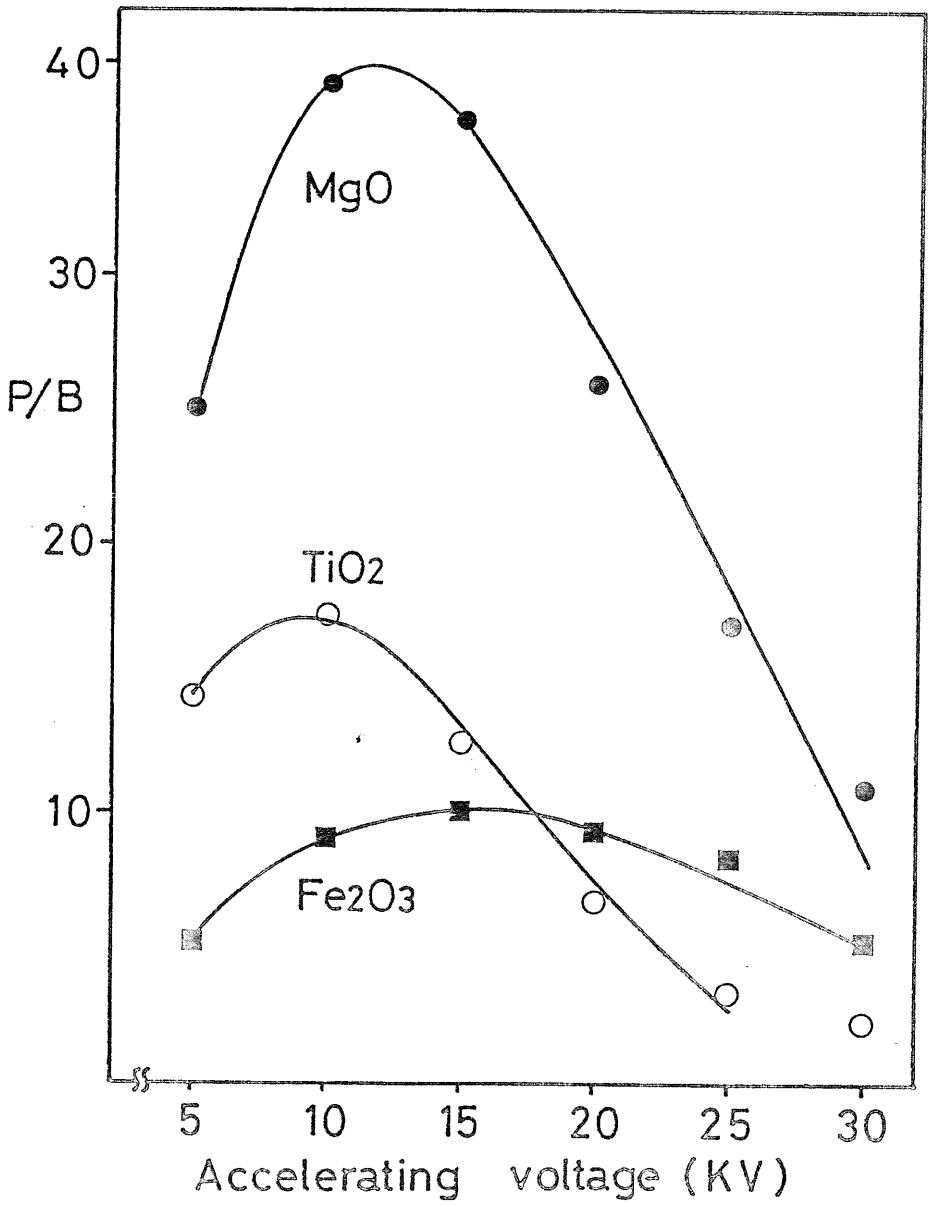

Fig. 2-10. P/B (P: peak intensity, B: background intensity) of OK_{α} line versus accelerating voltage for MgO, TiO_2 and Fe_2O_3.

Table 2-7. Measured X-ray intensity ratios of OK_α in double oxides using aluminium oxide standard

Sample	Accelerating voltage (kV)					
	5	10	15	20	25	30
MgO	0.812*	0.925	0.917	0.942	0.984	0.939
Cr_2O_3	0.753*	0.941	1.05	1.24	1.26	1.19
TiO_2	0.611*	0.360	0.264	0.265	0.240	0.231
Fe_2O_3	0.723*	0.822	0.849	0.914	0.951	0.884
NiO*	0.502	0.484	0.496	0.488	0.486	0.488
MoO_3*	0.541	0.351	0.271	0.254	0.263	0.253
ZrO_2*	0.483	0.299	0.233	0.212	0.208	0.211

* quoted from the results of Love et al. (1974b)

Table 2-8. RMS errors of oxygen analysis in binary oxide systems

Absorption correction	RMS error(%) of k'/k	
	5 - 30 kV	High P/B region*
Simple Philibert	11.5	7.91
Full Philibert	9.86	12.3
Yakowitz-Heinrich	20.4	8.38

* Accelerating voltage : 10, 15 kV

Atomic number correction : Duncumb-Reed equation

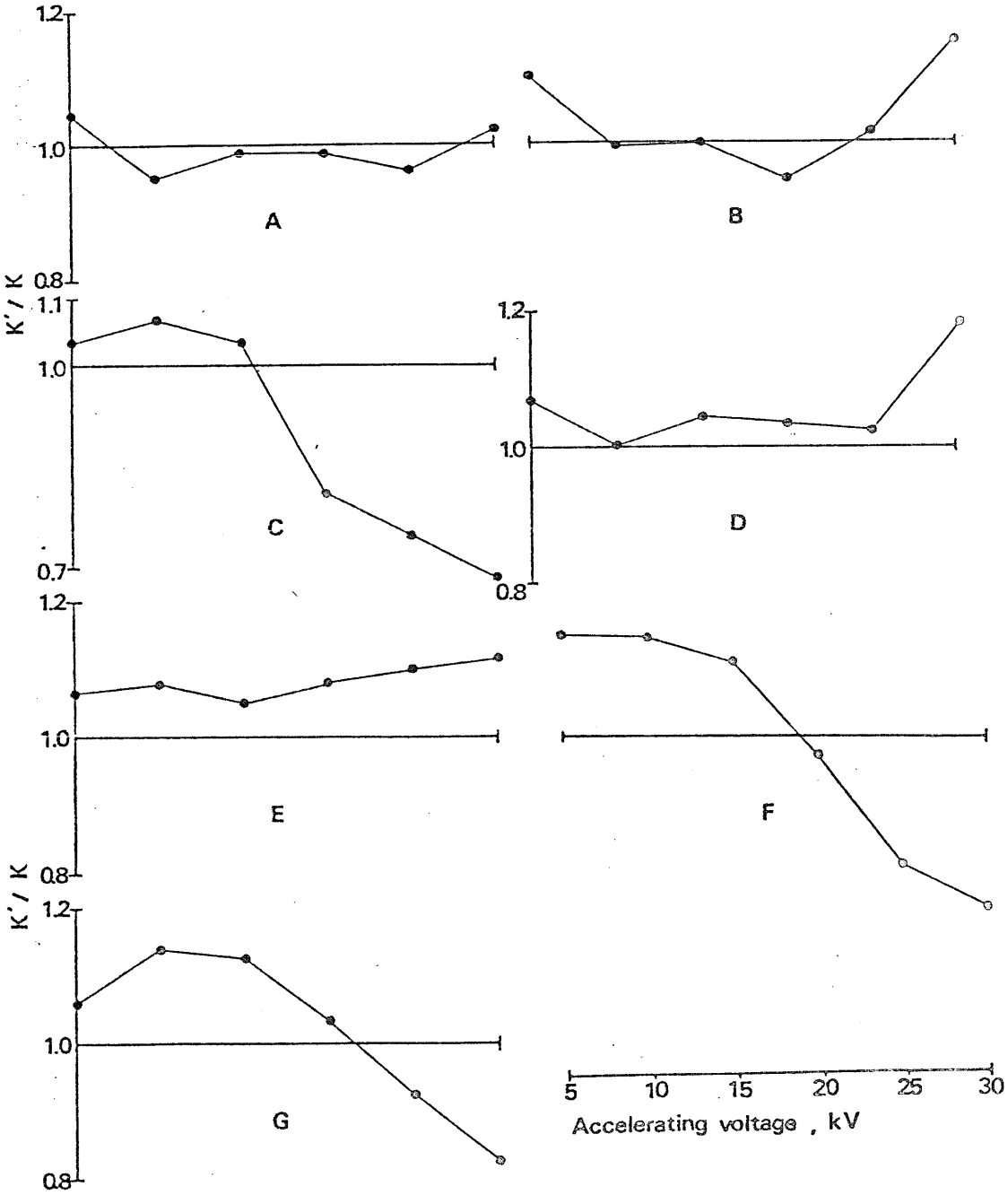

Fig. 2-11. Plots of k'/k using simple Philibert absorption correction together with Duncumb-Reed atomic number correction for MgO(A), Cr_2O_3(B), TiO_2(C), Fe_2O_3(D), NiO(E), MoO_3(F) and ZrO_2(G).

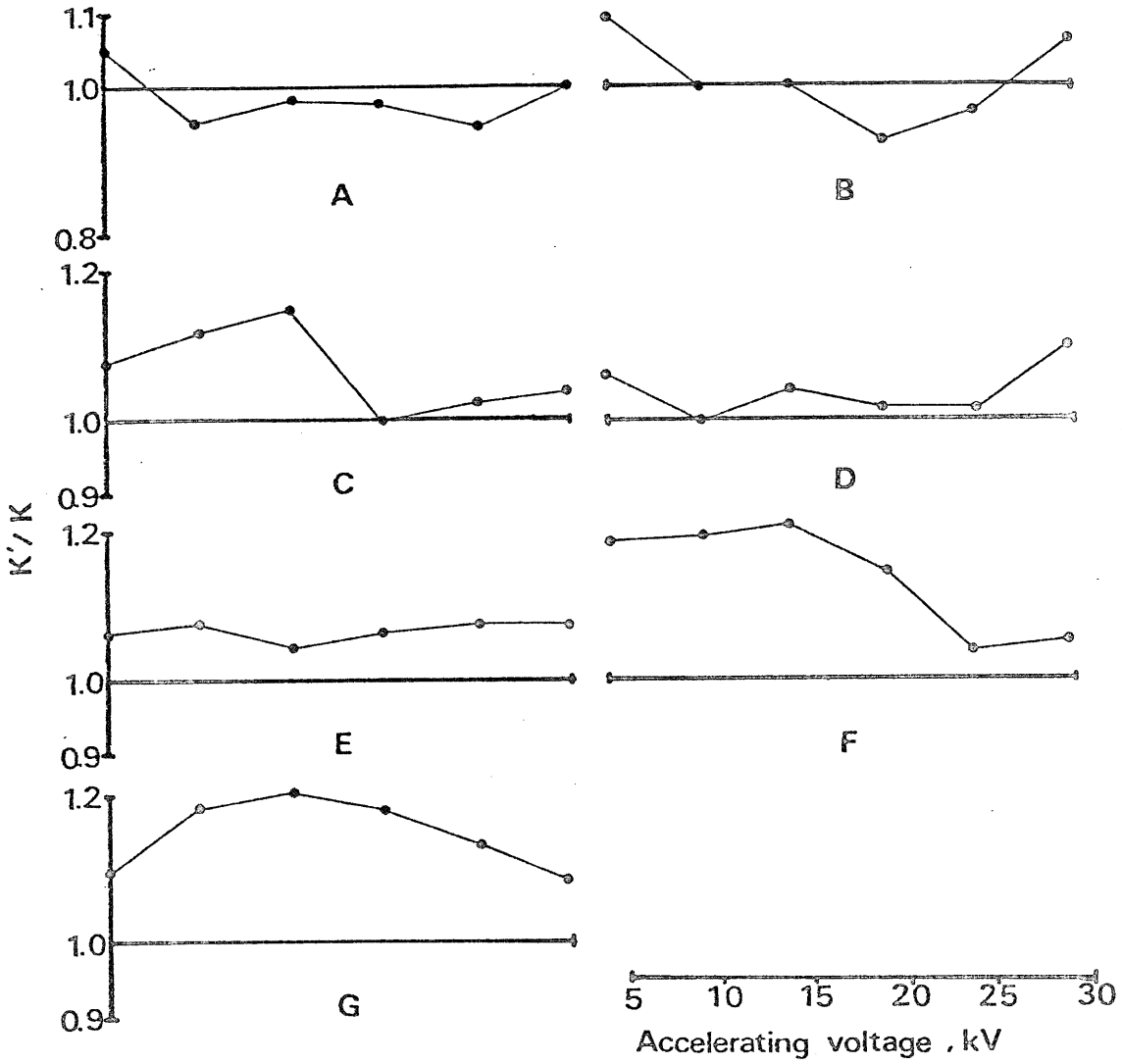

Fig. 2-12. Plots of k'/k using full Philibert absorption correction together with Duncumb-Reed atomic number correction for MgO(A), Cr_2O_3(B), TiO_2(C), Fe_2O_3(D), NiO(E), MoO_3(F) and ZrO_2(G).

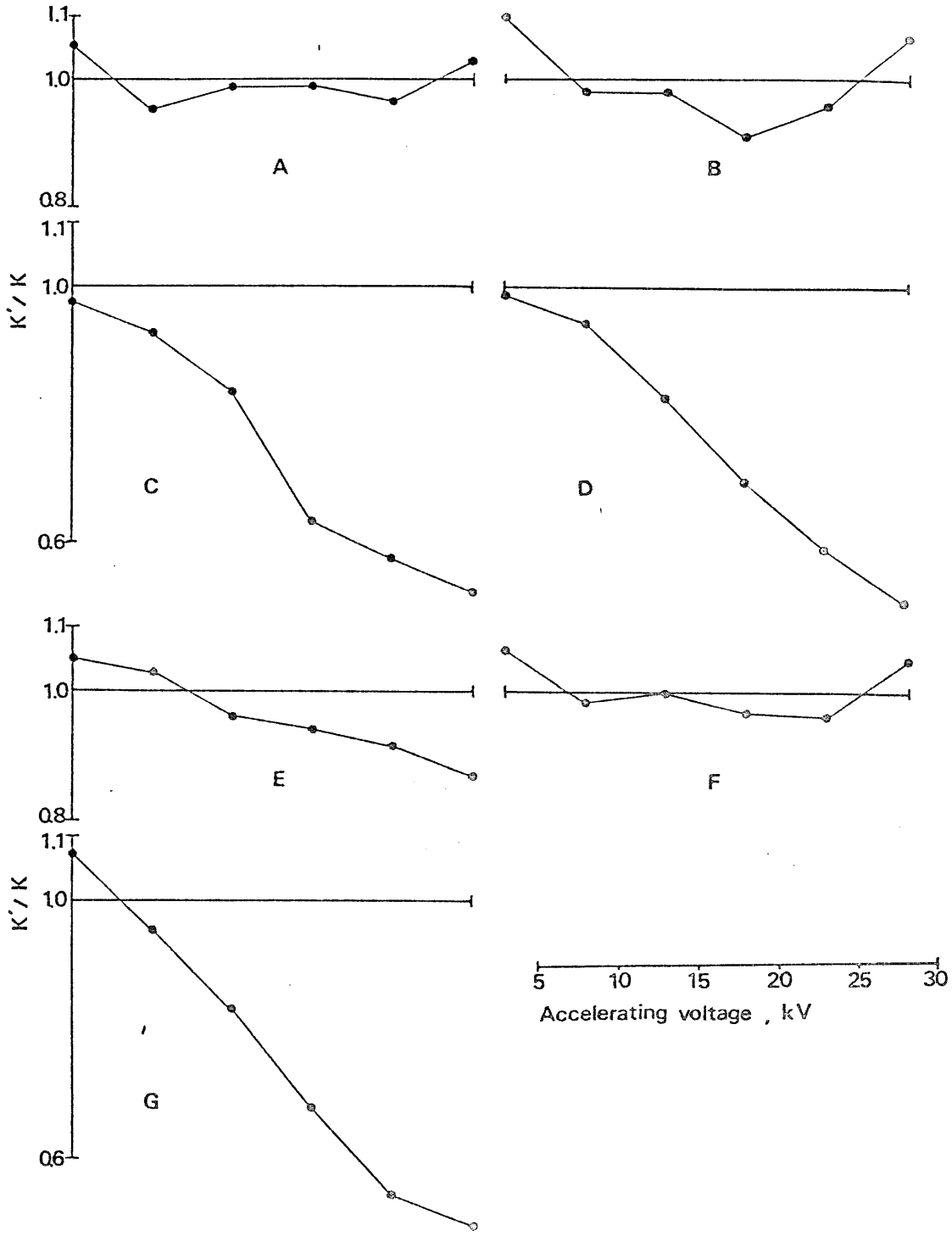

Fig. 2-13. Plots of k'/k using Yakowitz-Heinrich absorption correction together with Duncumb-Reed atomic number correction for MgO(A), Cr_2O_3(B), TiO_2(C), Fe_2O_3(D), NiO(E), MoO_3(F) and ZrO_2(G).

5. Silicate

5.1. Analytical Conditions and Samples

The measurement of OK_α in silicates, ie. SiO_2, $CaSiO_3$, $NaAlSi_3O_8$ and $KAlSi_3O_8$, were carried out at the accelerating voltage 5, 7, 10, 12, 15 , 20 and 25 kV. The details of analytical condition were similar to those described in section 2(double oxides of lanthanoid and niobium). The samples were synthetic SiO_2 and $CaSiO_3$ and natural $NaAlSi_3O_8$ and $KAlSi_3O_8$. The compositions of the latter two feldspars were confirmed by wet chemical analysis.

5.2. Results and Discussion

5.2.1. Examination of Analytical Condition

The P/B ratios of OK_α for silicates are shown in Fig. 2-14. This figure indicates the suitable accelerating voltage is in the range from 10 to 15 kV for oxygen analysis in silicates.

5.3. Examination of Absorption Correction

The observed x-ray intensity ratios of OK_α using almimiun oxide standard are listed in Table 2-9 as a function of accelerating voltage. The accuracy of analyses of silicates is shown in Table 2-10 by the RMS error. The ratios for k'/k using various absorption corrections together with Duncumb-Reed atomic number correction are shown in Fig. 2-15 (simple Philibert),

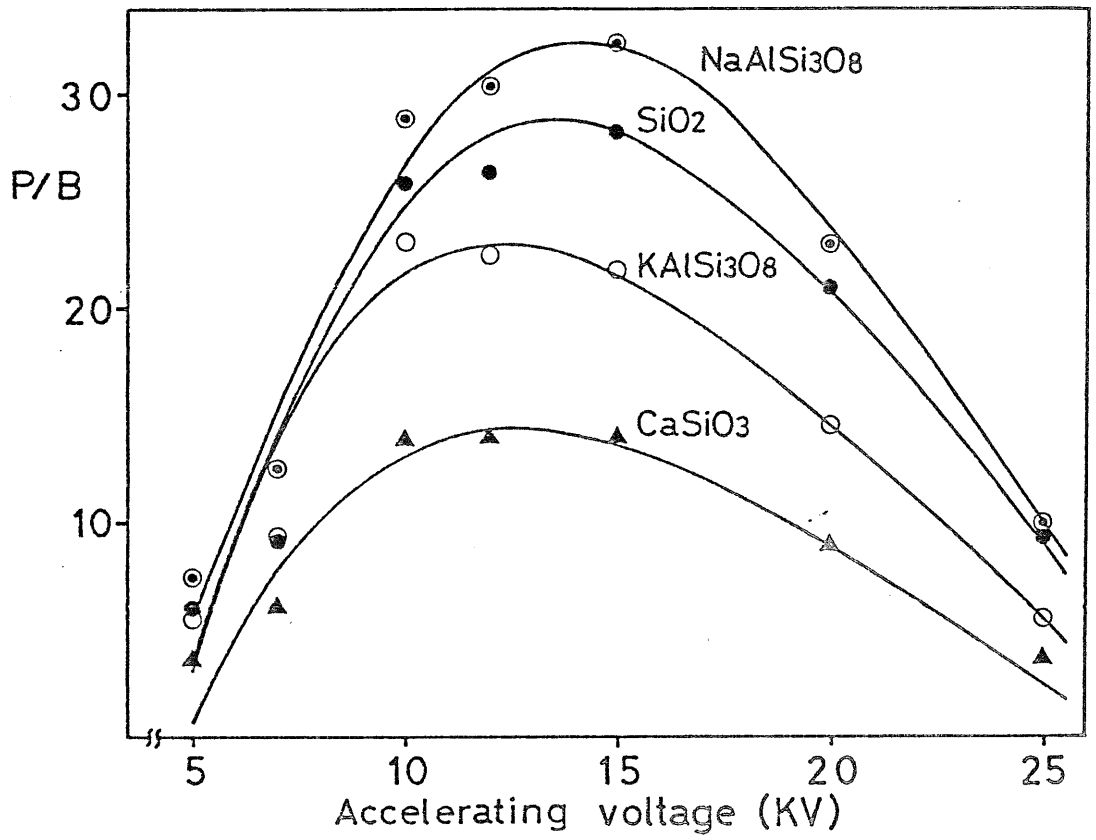

Fig. 2-14. P/B (P: peak intensity,B: background intensity) of OK_α line versus accelerating voltage for SiO_2, $CaSiO_3$, $NaAlSi_3O_8$ and $KAlSi_3O_8$.

Table 2-9. Measured X-ray intensity ratios of Ok_{α} in silicates using aluminium oxide standard

Sample	Accelerating voltage (kV) 5	7	10	12	15	20	25
SiO_2	1.01	1.02	1.02	0.970	0.947	0.926	0.900
$CaSiO_3$	0.646	0.567	0.459	0.409	0.373	0.345	0.326
$NaAlSi_3O_8$	1.01	1.00	0.990	0.993	0.978	0.954	0.956
$KAlSi_3O_8$	0.801	0.796	0.673	0.649	0.637	0.605	0.579

Table 2-10. RMS errors of oxygen analysis in silicates

Absorption correction	RMS error(%) of k'/k
Simple Philibert	6.01
Full Philibert	5.22
Yakowitz-Heinrich	9.30

Atomic number correction : Duncumb-Reed equation

2-16 (full Philibert), 2-17 (Yakowitz-Heinrich). In high P/B ratio range the simple Philibert absorption correction gave satisfactory results as shown in Fig.2-15. On the other hand the full Philibert absorption correction gave good results in high accelerating voltage range (20 and 25 kV) as shown in Fig. 2-16. This result may be due to the contribution of $\phi(0)$ term in the correction because the magnitude of the surface X-ray intensity $\phi(0)$ is increased according to increasing absorption effect.

6. Conclusion

Absorption correction and analytical condition for the quantitative electron microprobe analysis of oxygen in several binary oxide systems, silicates, sulfates and double oxides of lanthanoid and niobium have been investigated in the soft X-ray region.

The most suitable accelerating voltage for the practical oxygen analysis was in the range $10 \leq E_0 \leq 15$kV. The full Philibert absorption correction gave better results in the oxygen analysis than those of the simple Philibert or the Yakowitz-Heinrich correction because of the contribution of $\phi(0)$ term in the high accelerating voltage range. However even the full Philibert absorption correction did not give satisfactory results to all measured accelerating voltage and samples. For example,

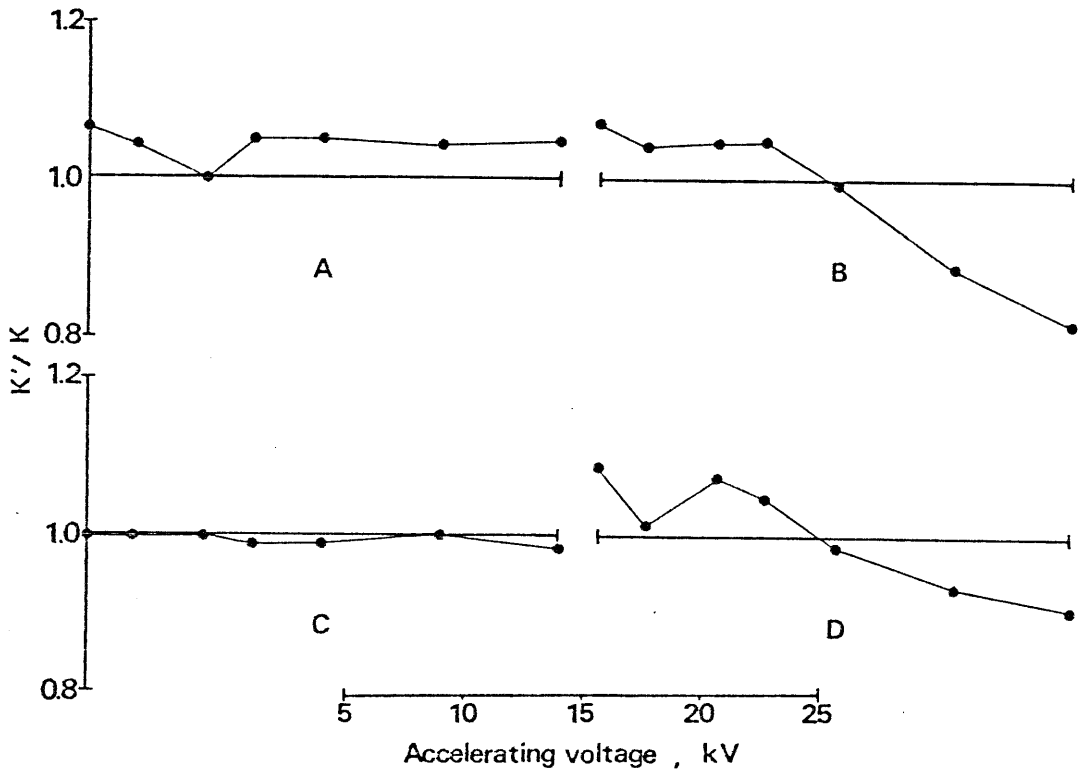

Fig. 2-15. Plots of k'/k using simple Philibert absorption correction together with Duncumb-Reed atomic number correction for SiO_2(A), $CaSiO_3$ (B), $NaAlSi_3O_8$(C) and $KAlSi_3O_8$(D).

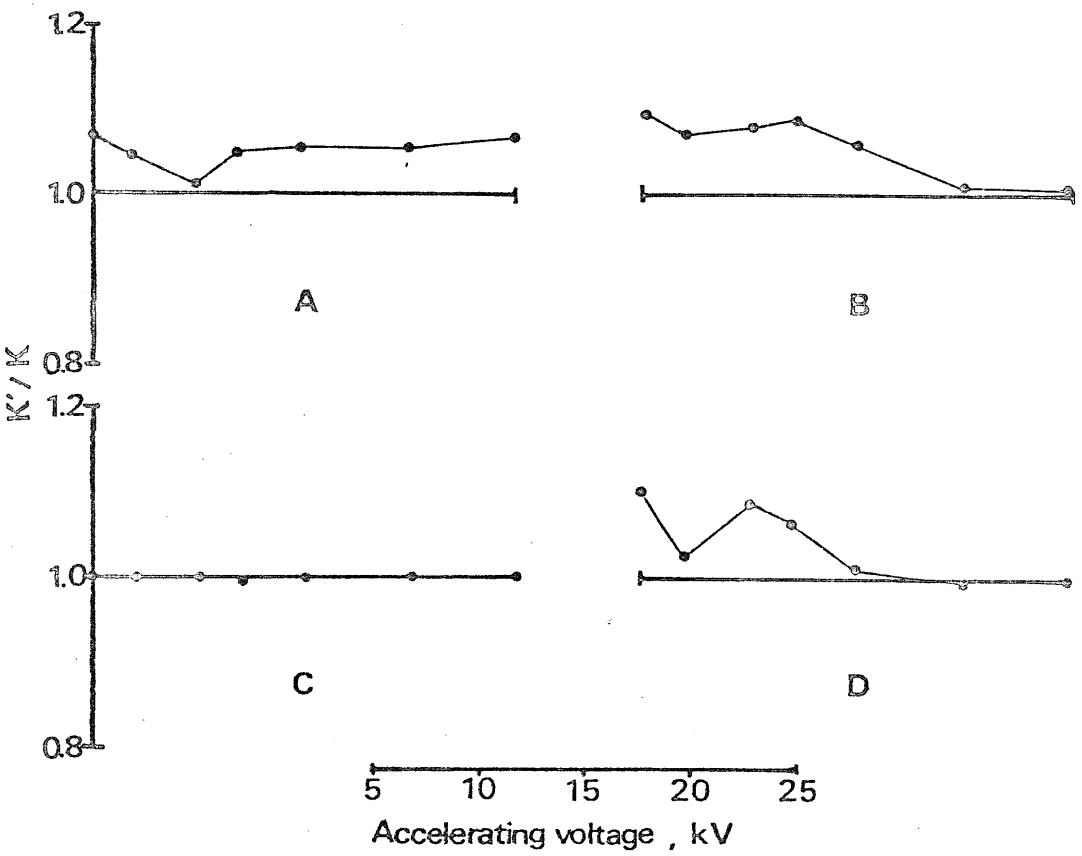

Fig. 2-16. Plots of k'/k using full Philibert absorption correction together with Duncumb-Reed atomic number correction for SiO_2(A), $CaSiO_3$(B), $NaAlSi_3O_8$(C) and $KAlSi_3O_8$(D).

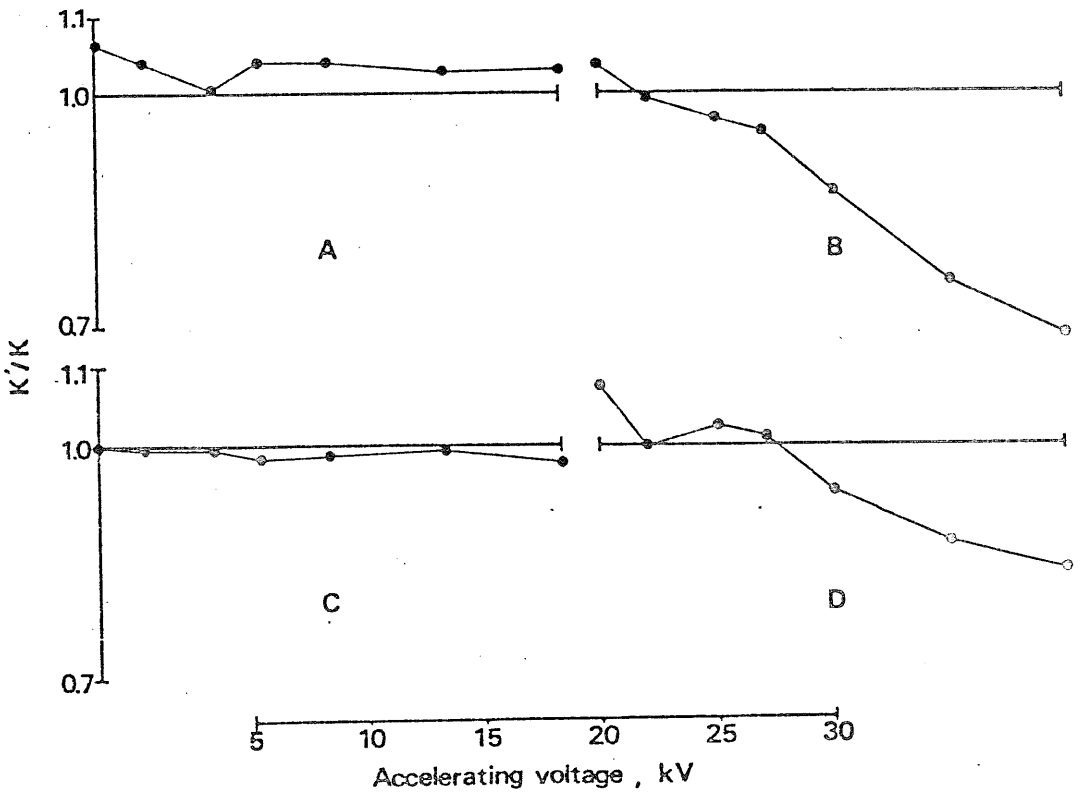

Fig. 2-17. Plots of k'/k using Yakowitz-Heinrich absorption correction together with Duncumb-Reed atomic number correction for SiO_2(A), $CaSiO_3$(B), $NaAlSi_3O_8$(C) and $KAlSi_3O_8$(D).

the correction gave good results in silicates and double oxides of lanthanoid and niobium, but gave large RMS errors (more than 10%) on oxygen analysis in sulfates and several binary oxides. As a conclusion, an improved absorption correction is required for quantitative light elements analysis.

Chapter 3. New Absorption Correction

1 Introduction

To obtain quantitative results in electron probe microanalysis, corrections must be made on the electron penetration and backscattering (atomic number correction:Z), absorption (:A) and fluorescence effect (:E). Among them the absorption correction is the most important. And, as already mentioned, there is no effective absorption correction equation especially for the analysis of light elements because of larger absorption effect on these elements.

In order to establish a new absorption correction, it is necessary to make clear of the ionization distribution along depth, ρz, of primary X-rays. The absorption correction is expressed as

$$f(\chi) = \frac{\int_0^\infty \phi(\rho z)\exp(-\chi\rho z)\,d(\rho z)}{\int_0^\infty \phi(\rho z)\,d(\rho z)}$$

where $\phi(\rho z)$ is the distribution of ionization, and $\chi = (\mu/\rho)\mathrm{cosec}\,\theta$, where μ/ρ is the mass absorption coefficient and θ is the X-ray take-off angle. By expanding the exponential term as a power series, this equation can be written (Bishop 1974) as

$$f(\chi) = 1 - \chi \frac{\int_0^\infty \rho z \phi(\rho z) d(\rho z)}{\int_0^\infty \phi(\rho z) d(\rho z)} = 1 - \chi \cdot \overline{\rho z}$$

where $\overline{\rho z}$ is called "mean depth of ionization". And by expressing $f(\chi)$ as a Maclaurine series, that is written as

$$f(\chi) = \frac{\phi(0)}{\chi} \frac{1}{\int_0^\infty \phi(\rho z) d(\rho z)} .$$

The former equation, which is dependent on the mean depth $\overline{\rho z}$ and χ, may be expected to hold good approximation in the range $0.8 \leq f(\chi) \leq 1.0$. The simple Philibert equation gives good analytical results in this range because it predicts accurate mean depth $\overline{\rho z}$ (Bishop 1974). The latter equation, derived after the thin-film model initially introduced by Duncumb and Merford (1966), is dependent on the two parameters, surface ionization function $\phi(0)$ and χ, and could be applied to the analysis when $f(\chi)$ is less than about 0.01. In the range $0.01 \leq f(\chi) \leq 0.8$ above absorption correction equation is dependent on the shape of ionization distribution and there is no effective correction equation in this range. Therefore, light elements analysis requires an improved absorption correction in this lower range.

The $\phi(\rho z)$ has been determined commonly by the two methods, one is an experimental method called "tracer method" and another is theoretical method called "Monte Carlo method". As both of these two methods have several weak points, they often give the different $\phi(\rho z)$ curves. Therefore, it can not be decided which $\phi(\rho z)$ curve should be used to make a new absorption correction. Then the author proposed two absorption corrections in this chapter, the one, based on the experimental $\phi(\rho z)$ determined tracer technique, and theoretical $\phi(\rho z)$ determined by the Monte Carlo method respectively.

2. An Improved Absorption Correction Based on Wittry's Ionization Distribution

Several ionization distributions, ie. Philibert, square and Gaussian model, are shown in Fig. 3-1. Love et al. (1974) concluded that the full Philibert absorption correction gave better results for oxygen analysis in some binary and ternary oxide systems than the correction based on the Wittry's Gaussian ionization distribution. The absorption correction associated with this model must give good analytical results in lower $f(\chi)$ region because the shape of Gaussian fits closely to the one determined by Monte Carlo method as shown in Fig. 3-1.

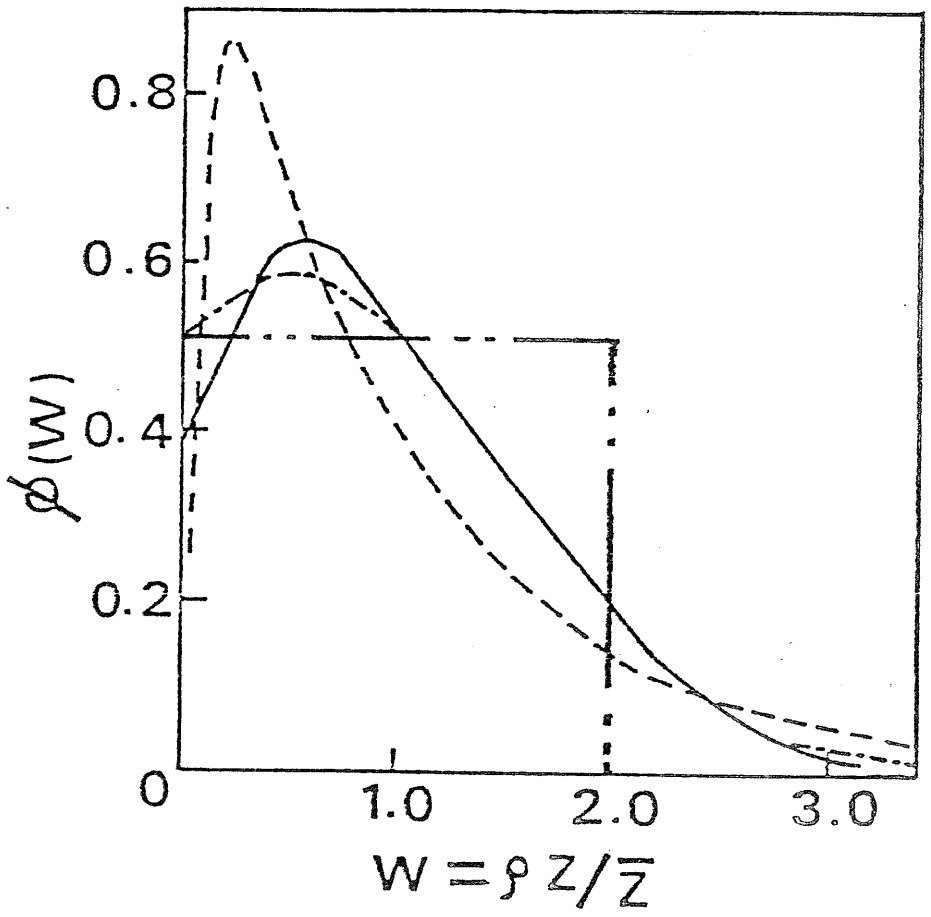

Fig. 3-1. Normalized ionization distribution in a copper matrix for an overvoltage ratio U=10: —— Monte Carlo, ------ Gaussian, ----- Philibert ------- square model.

2.1. Theory and Calculation

The Gaussian ionization distribution, initially introduced by Wittry(1957) is expressed as

$$\phi(\rho z) = A \exp\left\{ -\left(\frac{\rho z - \rho z_o}{\rho \Delta z} \right)^2 \right\}$$

The absorption correction equation $f(\chi)$ can be obtained from the above equation by Laplace transform. Then, the $f(\chi)$ can be described by the following equation.

$$f(\chi) = \frac{\exp(-b^2).\exp(u^2)\cdot \mathrm{Erfc}(u)}{1 + \mathrm{Erf}(b)}$$

where $u = q\chi - b$, $b = \frac{5}{14}$, and q is proportional to the electron range R.

The value of q could be determined from $f(\chi)_{obs}$ data, which are calculated from experimental $\phi(\rho z)$, by least square curve fitting method. The experimental $f(\chi)_{obs}$ data are calculated from the experimental $\phi(\rho z)_{obs}$ by the following equation.

$$f(\chi)_{obs} = \frac{\int_o^\infty \phi(\rho z)_{obs} \exp(-\chi \rho z) d(\rho z)}{\int_o^\infty \phi(\rho z)_{obs} d(\rho z)}$$

The experimental $\phi(\rho z)$ of Au, Ag, Ni, Al and Cu target at the accelerating voltage 6,8,10,15,20,25 and 30 kV using various tracer were used and were determined

by Brown et al. (1972,1975,1978,) and Parobek (1972) using the sandwitch technique.

The $f(\chi)_{obs}$ values used were about 30 points for each ionization distribution in the range $0.08 \leq f(\chi) \leq 1.0$. A computer program of SALS system (by Oyanagi and Nakagawa) was used in the calculation of the least square curve fitting with robust estimation.

2.2. Results and Discussion

Calculated results of q by nonlinear least square curve fitting are listed in Table 3-1. The 0.02 error range has been assumed throughout the calculation on each point. At this stage, it is interesting to examine the ratio $f(\chi)/f(\chi)_{obs}$ of this model and that of commonly used Philibert model.

Several $f(\chi)/f(\chi)_{obs}$ curves, ie.Au,Al,Ag, etc., at accelerating voltage 30, 20 and 10 kV are shown in Figs.3-2,3 and 4 respectively. These figures show that the values predicted by these models agreed approximately with the experimental values in the range $0.8 \leq f(\chi)$. Therefore these equations may be expected to predict an accurate mean depth of ionization, and give good analytical results in ordinary analysis. However, the values predicted by the Philibert model are in complete disagreement with the experimental data in the $f(\chi) < 0.8$ region. The deviation from the experimental values may be attributed to the use of incorrect shape function in the Philibert model. The assumption appeared in the model $\phi(0) = 0$, is apt to give serious error against the $f(\chi)_{obs}$ in the low $f(\chi)$ region.
On the other hand, the Gaussian model can be expected to predict precise values in the range $1.0 \leq f(\chi) \leq 0.2$ because its shape function is similar to the one

Table 3-1 Calculated results of q (mg/cm^2) by least square curve fitting method

Matrix	Tracer	Accelerating voltage (kV)	q (mg/cm^2)	Res.*
Al	BiLα	30	0.326_7	2.87×10^{-3}
Cu	BiLα	30	0.338_2	1.64×10^{-3}
Au	BiLα	30	0.342_6	9.39×10^{-3}
Ag	BiLα	30	0.320_3	2.99×10^{-3}
Al	BiLα	25	0.229_8	5.90×10^{-4}
Cu	BiLα	25	0.237_3	2.28×10^{-3}
Ag	BiLα	25	0.220_2	3.16×10^{-3}
Au	BiLα	25	0.260_4	8.64×10^{-3}
Al	ZnKα	25	0.245_9	1.27×10^{-3}
Cu	ZnKα	25	0.238_0	8.14×10^{-4}
Ag	ZnKα	25	0.242_9	5.09×10^{-3}
Al	CdLα	25	0.311_8	5.00×10^{-3}
Cu	CdLα	25	0.249_4	2.57×10^{-3}
Ag	CdLα	25	0.289_4	1.17×10^{-3}
Au	CdLα	25	0.276_1	3.99×10^{-3}
Al	BiLα	20	0.121_4	1.51×10^{-3}
Ag	BiLα	20	0.133_6	5.13×10^{-3}
Cu	BiLα	20	0.133_0	3.65×10^{-3}
Au	BiLα	20	0.168_5	8.21×10^{-3}
Al	BiMα	15	0.123_0	3.17×10^{-3}
Cu	BiMα	15	0.126_5	1.11×10^{-3}
Ag	BiMα	15	0.122_7	2.07×10^{-3}
Au	BiMα	15	0.148_1	2.01×10^{-3}
Ni	Cukα	15	0.093_8	2.41×10^{-3}
Ni	CuKα	12	0.056_2	3.23×10^{-3}
Al	SiKα	10	0.061_6	2.09×10^{-3}
Ni	SiKα	10	0.064_1	1.97×10^{-3}
Ag	SiKα	10	0.071_4	3.67×10^{-3}
Au	SiKα	10	0.081_4	5.96×10^{-3}
Al	SiKα	8	0.041_6	1.76×10^{-3}
Ni	SiKα	8	0.042_9	3.20×10^{-3}
Ag	SiKα	8	0.048_6	4.75×10^{-3}
Au	SiKα	8	0.056_1	6.54×10^{-3}
Al	SiKα	6	0.024_1	2.81×10^{-3}
Ni	SiKα	6	0.025_0	4.61×10^{-3}
Ag	SiKα	6	0.027_7	7.52×10^{-3}
Au	SiKα	6	0.034_1	9.27×10^{-3}

*Res. $= \sqrt{\Sigma (f(\chi)_{obs} - f(\chi)_{cal})^2 / n}$

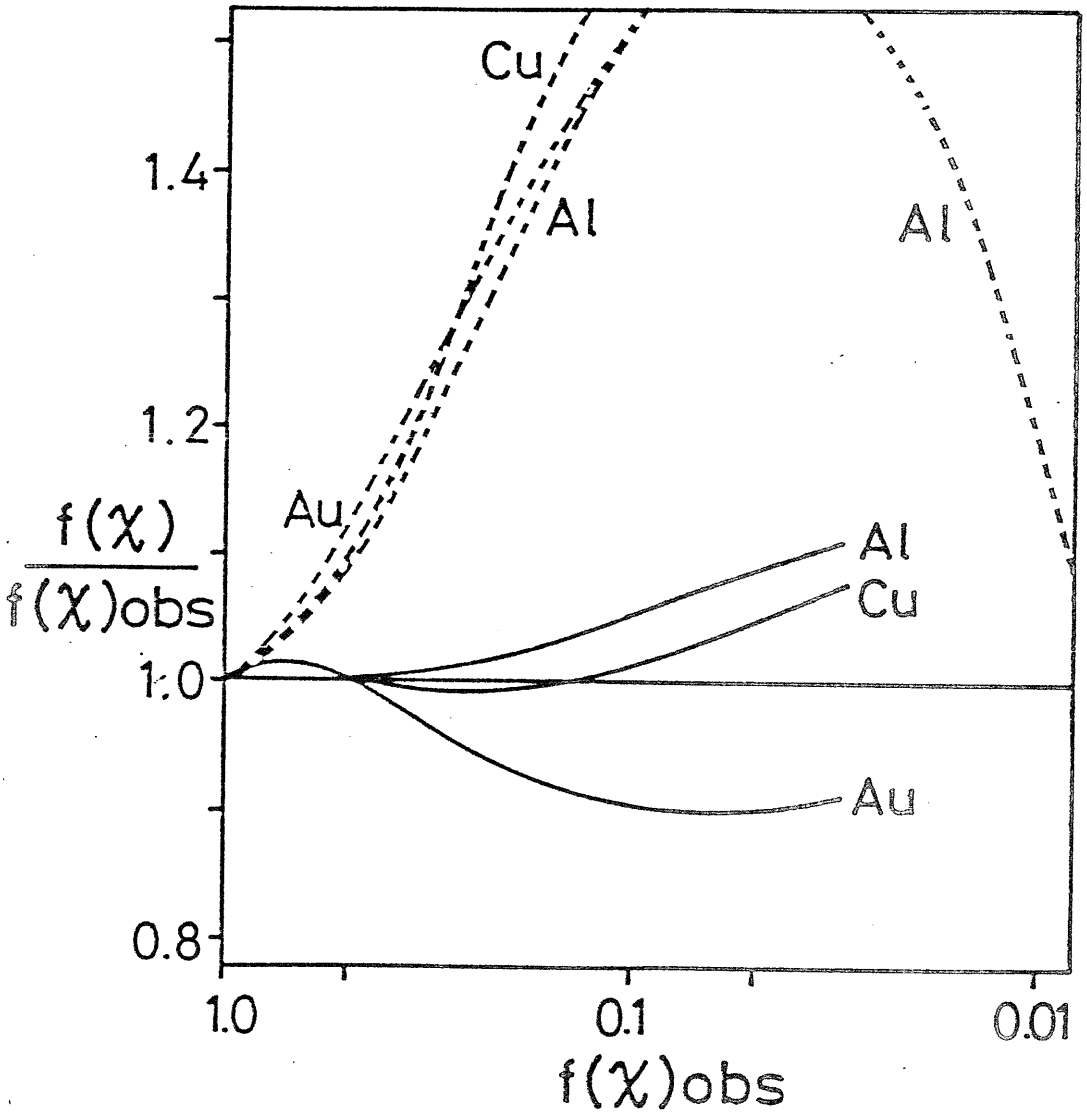

Fig. 3-2. Ratio of $f(\chi)/f(\chi)_{obs}$ using experimental ionization distribution for 30 kV (Bi tracer).
——— Gaussian model, ----- Philibert model.

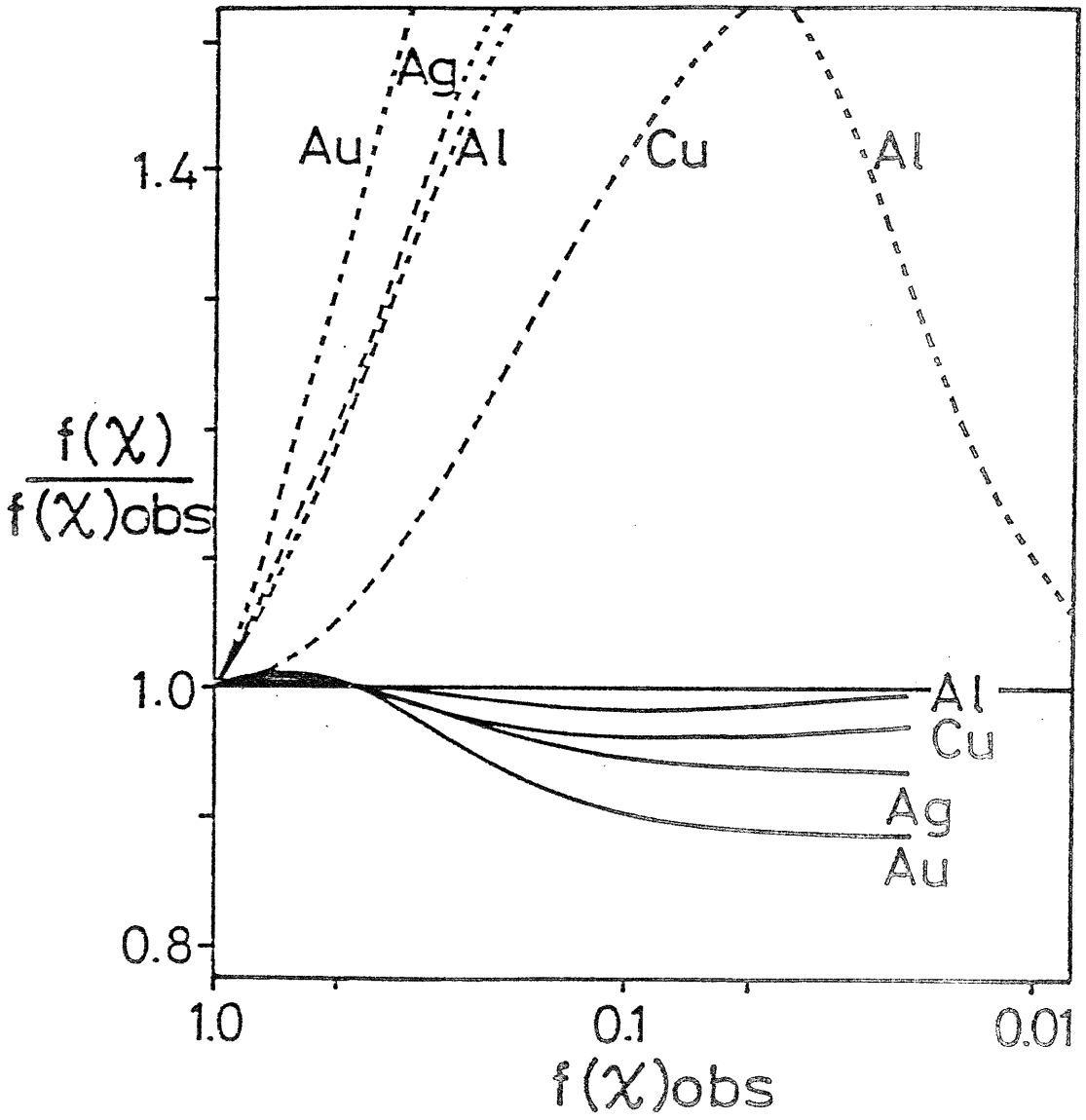

Fig. 3-3. Ratio of $f(\chi)/f(\chi)_{obs}$ using experimental ionization distribution for 20 kV (Bi tracer).
——— Gaussian model, ----- Philibert model.

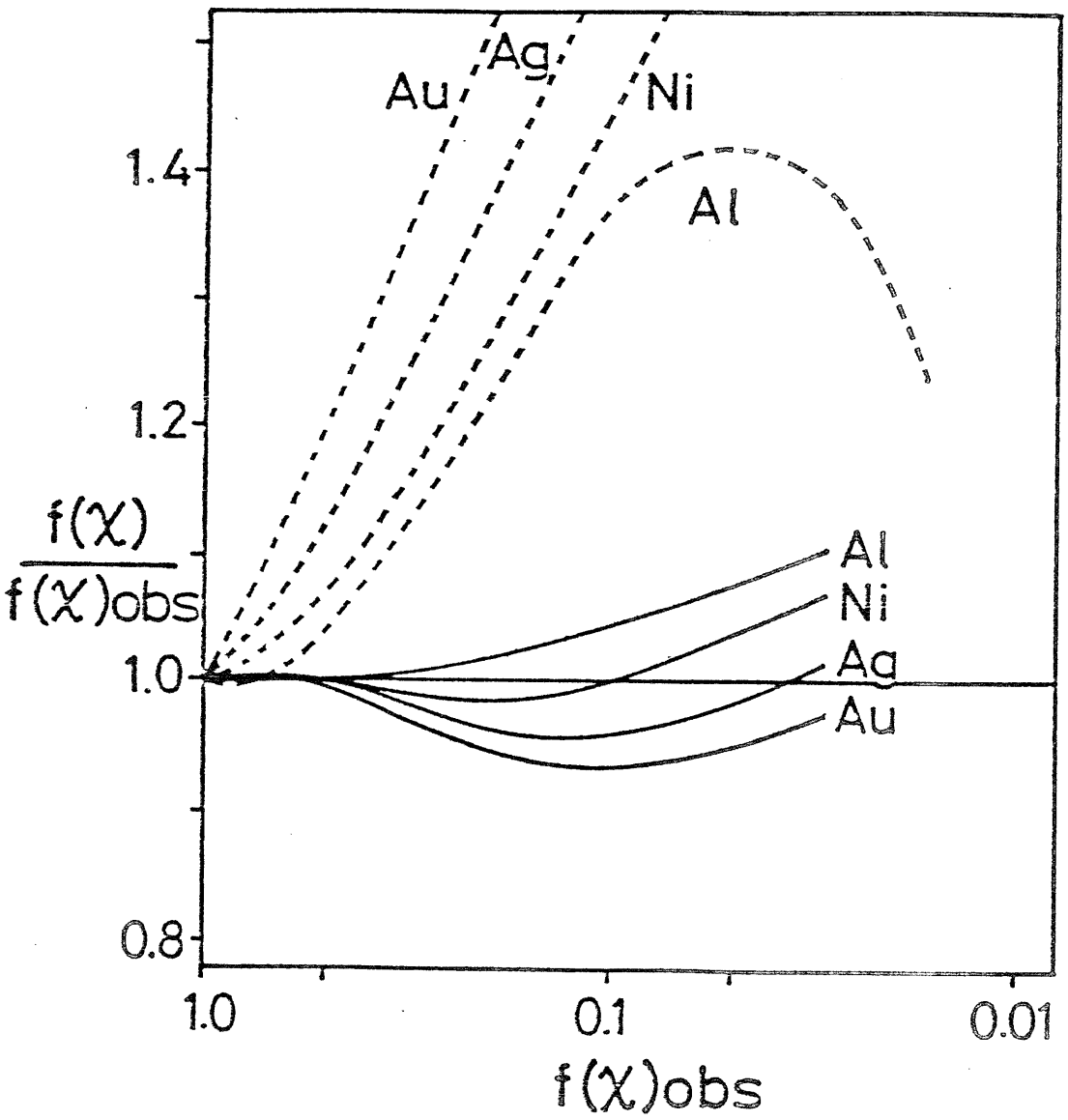

Fig. 3-4. Ratio of $f(\chi)/f(\chi)_{obs}$ using experimental ionization distribution for 10 kV (Si tracer).
——— Gaussian model, ----- Philibert model.

determined by Monte Calro method. Unfortunately the influence of mean atomic number effect is brought out clearly in Fig. 3-2. The effect, however, is not a serious problem in the practical analysis because it is rather smaller than the other factors in the lower $f(\chi)$ region. As the Gaussian $\phi(\rho z)$ does not predict $\phi(0)$ value correctly, the absorption corretion associated with this model predicts somewhat inaccurate values for the range $f(\chi) < 0.2$.

Because the range $0.2 \leq f(\chi) \leq 1$ includes the analysis region of most elements even for oxygen analysis, the $f(\chi)$ values in this range is important in practical analysis. The variation of this equation and the experimental $f(\chi)$ data in the range $0.2 < f(\chi) < 0.05$ is not so large (within 10%). On the other hand, Philibert model gave very large variation in the range $f(\chi) < 0.8$. Therefore, the equation based on the Gaussian ionization distribution is expected to give good results of analysis because this equation is in good agreement with experimental $f(\chi)$ data in wide range.

2.2.1. The Equation q

The equation q is related to the electron range R. When the ionization distribution is expressed as $\phi(\rho z) = A \exp\{-(\frac{\rho z - z_o}{\rho \Delta z})^2\}$, q is written as follows.

$$q = \frac{\rho \Delta z}{2} = \frac{0.35}{2} R.$$

Andersen-Wittry (1968) and Kyser (1972) gave the following values for R.

$$R = 2.56 \times 10^{-3} \ (\ g/cm^2) \qquad \text{(Andersen-Wittry)}$$

$$R = 2.56 \times 10^{-3} (E_0/30)^{1.68} \ (\ g/cm^2) \qquad \text{(Kyser)}$$

The constants 2.56×10^{-3} appeared in the both equations were determined from the energy versus depth of electron penetration in a Cu target at 30 kV based on transport equation calculation. As neither Kyser nor Andersen-Wittry consider the effect of matrix elements on thier equation, the R values remain constant under any condition of E_0 even on the equation of Kyser. Calculated results of q by least square curve fitting are affected by the atomic number of matrix element and accelerating voltge as shown in Table 3-1. As q is proportional to R, it may be related to the Bethe range or extrapolated range of electrons.

In general R obeys simple scaling law ($R \propto E_0^n$). Different values are given to the power n on E_0 according to the definition of R. The equation q may be expressed as

$$q = a(E_0^n - E_c^n) \cdot g(h) \ ,$$

where, g(h) represents the atomic number effect. On the Bethe equation for electron energy loss, the variation caused by the atomic number effect is expressed by Z/A term and J (mean ionization potential). Since electron range R is proportial to the reciprocal of the Bethe equation, g(h) term may be expressed as A/Z^n generally. Considering these factors the author assumed the following equation,

$$q = a(E_o^n - E_c^m) \cdot A/Z^p \qquad (I)$$

or

$$q = a\, E_o^n \left(1 - \left(\frac{E_c}{E_o}\right)^m\right) A/Z^p \qquad (II)$$

where n is not always necessary equal to m although the equations commonly used as n = m.

The author determined the a,n,m and q by the non-linear least square curve fitting method with robust estimation using above equations. According to the calculated results, following equations are obtained;

i) $$q = 1.158 \times 10^{-6}(E_0^{1.59} - E_c^{1.33})A/Z^{1.1} \ g/cm^2 \qquad (I)$$

$$R = 2.027 \times 10^{-6}(E_0^{1.59} - E_c^{1.33})A/Z^{1.1} \qquad (II)$$

ii) $$q = 8.6 \times 10^{-7}\, E_0^{1.53}\left(1-\left(\frac{E_c}{E_0}\right)^{3.16}\right)A/Z \ g/cm^2 \qquad (III)$$

$$R = 1.505 \times 10^{-7} E_0^{1.53}\left(1-\left(\frac{E_c}{E_0}\right)^{3.16}\right)A/Z \qquad (IV)$$

In the equation (II), the calculation was done using following relation in order to reduce the parameter.

$$q.(Z/A) = a \cdot E_0^n \ (1-(E_c/E_0)^m).Z^{p'}$$

In the R equation the power of E_0 and E_c is expressed as n = m in general,but the equation q does not hold same scale in E_0 and E_c. If this calculation would be done under the condition n = m, the equation q obtained would give large error against the q values in Table 3-1.

2.2.2. Property of Electron Range Associated with Gaussian Ionization Distribution

There are various equations about the electron range according to the definition of it. The power on E_0 in equation (II) are in close agreement with the values derived from extrapolated range, n = 1.5 for copper, silver and gold in the range from 5 to 15kV, determined by Cosselet and Thomas (1966) for beam energy loss., which is corresponding to the mean depth of 96-98 % loss in incident beam energy.

On the other hand, Bethe range, which is corresponding to the total path length, is determined experimentally to be in the region 1.7-1.8. In a lower energy region ($E \leq 6.388J_i$, where J_i is mean ionization potential of element i), the Bethe equation can be

modified as (by Rao-Sahib-Wittry, 1974).

$$-\frac{dE}{d\rho s} = \frac{7.85\times 10^4}{1.26\ E}\ \Sigma\ \frac{C_i Z_i}{A}\ \frac{1}{J}\ .$$

According to this equation, the range R is expressed as follows.

$$R = \rho S = \alpha\ E^{1.5}\ \Sigma\ \frac{A_i \cdot \bar{J}_i}{C_i Z_i} \qquad \text{where, } \alpha \text{ is constant.}$$

The power of 1.5 on E agrees with the value in equation (III). The power value 1.59 in equation (II) is within the region of the Bethe and the extrapolated range.

In order to calculate the electron range, it is usually assumed that the differential dR/dE is the reciprocal of the stopping power. Therefore the range R of an electron from initial energy E_0 to critical excitation energy E_c along its trajectory may be determined from the following integration :

$$R = \int_{E_o}^{E_c} (-\frac{dR}{dE})\,dE = \int_{E_c}^{E_o} \frac{1}{S}\,dE\ ,$$

and the range R may be represented in the general form;

$$R = a(E_0^n - E_c^n)$$

Therefore, the power value on E_0 and E_c are equal.

However the q equation obtained in this chapter shows that the value n on E_0 is in complete disagreement with m on E_c. The reason is that an electron of energy E close to E_c cannot suffer an energy loss in excess of E_0-E_c, and the mean rate of energy loss is less than that predicted by the Bethe's law which assums that all energy losses are possible. The power n on E , therefore, may change into the power m on E_c according to decreasing the energy of electron because the energy loss is not continuous process but occurs in discreate steps. On the other hand, the power m on E_c agrees with the result (n = 1.3) of X-ray production range determined by Reuter (1978) in a lower energy level ($2 \leq E \leq 15$ kV). Taking above facts into consideration, the power n on accelerating voltage changes from 1.59 on E_0 to 1.33 on E_c according to the energy loss of electron because the energy loss are not continuous process.

2.2.3 Examination of Equation q

In order to find the best equation q for the practical analysis, absorption correction equation $f(\chi)$ associated with q were applied to the binary alloy systems ($Z \geq 12$) together with Pool-Thomass atomic number correction (1962).

The 150 analysis data determined by Pool (1968)

were used. The RMS errors obtained by equation q(I) and (II) were the same (5.67%).
As this value is much better than the results by commonly used Philibert model there is no problem on absorption correction using each equation q for practical analysis.

3. An Absorption Correction Based on a New Ionization Distribution

The shape of ionization distribution $\phi(\rho z)$ depends on the following four factors : the mean atomic number of the target (z), the incident beam energy (E), the critical ionization potential (E_c), and the overvoltage variation (U). However, Bishop indicated that overvoltage and accelerating voltage variation can be neglected for practical analysis using normalized ionization function $\phi(w)$, and consequently the shape may be affected by the mean atomic number effect only.

The $\phi(\rho z)$ determined by the tracer method is complicated by fluorescence effect and by the possibility of experimental error, and fluorescence affect, which is produced deeper in the target than the primary ionization distribution in general, is difficult to correct properly. In addition, the depth distribution of indirect ionization does not have the same dependence

on E as the primary ionization, which again must lead to the error. On the other hand, $\phi(\rho z)$ determined by the Monte Carlo method also have some problems.

A new $\phi(w)$ was built in order to obtain the new $f(\chi)$ equation using the data in a Cu target at 30 kV and U = 10 determined by the Monte-Carlo method (by Bishop 1974), since the $\phi(w)$ data was in fair agreement with experimental data.

3.1. Theory and Calculation

The following equation is assumed for normarilized shape function.

$$\phi(w) = A \exp(-a^2(w-b)^2 - B(\exp(-c^2w^2)), \quad (I)$$

where the latter term is the correction term for $\phi(0)$ value , and $w = \frac{\rho z}{\overline{\rho z}}$ and the $\overline{\rho z}$ is the mean depth of ionization.

The parameter A,B,a,b and c were decided by the nonlinear least square curve fitting using SALS system (Nakagawa and Oyanagi). The $\phi(w)$ data used are determined by Bishop (1974) in a Cu target at 30 kV and U = 10 with Monte Carlo method. The absorption correction equation $f(\chi)$ which can be derived from the $\phi(w)$ are written as

$$f(\chi') = \int_0^\infty \phi(w) \exp(-\chi' w)\, dw ,$$

where $\chi' = \chi\overline{\rho z}$, so that $\int_0^\infty \phi(w)dw = \int_0^\infty w\phi(w)dw = 1.0$. (2)

3.2. Results and Discussion

From the conditions shown by equation (2), the factors in equation (I) are required to satisfy the following equations.

$$A\{\frac{1}{2a^2} e^{-a^2b^2} + \frac{\pi}{2a}(1 + Erf(ab))\} - \frac{B}{2c^2} = 1.0$$

$$A \frac{\pi}{2a}(1 + Erf(ab)) - \frac{\pi}{2c^2} = 1.0$$

After deciding these factors (A,B,a, and b), the following normalized ionization function $\phi(w)$ was obtained.

$$\phi(w) = 0.664 \cdot \exp(-0.665^2(w - 0.3)^2 - 0.2 \cdot \exp(-3.23^2 w^2) \quad (3).$$

These factors, however, did not satisfy above equations completely because above $\phi(w)$ is an approximate equation. The $\phi(w)$ obtained in the present work is shown in Fig 3-5 together with the one given by Monte Carlo method. These curves coincide quite well in their shape in all region. And the $\phi(0)$ value predicted by the equation (3) agrees with the $\phi(0)$ value determined by the Monte Carlo method than those of Philibert or Wittry model (see Fig. 3-1). Therefore, the $f(\chi)$ equation assosiated with the $\phi(w)$ may be expected to give the accurate $f(\chi)$ value in a very wide range.

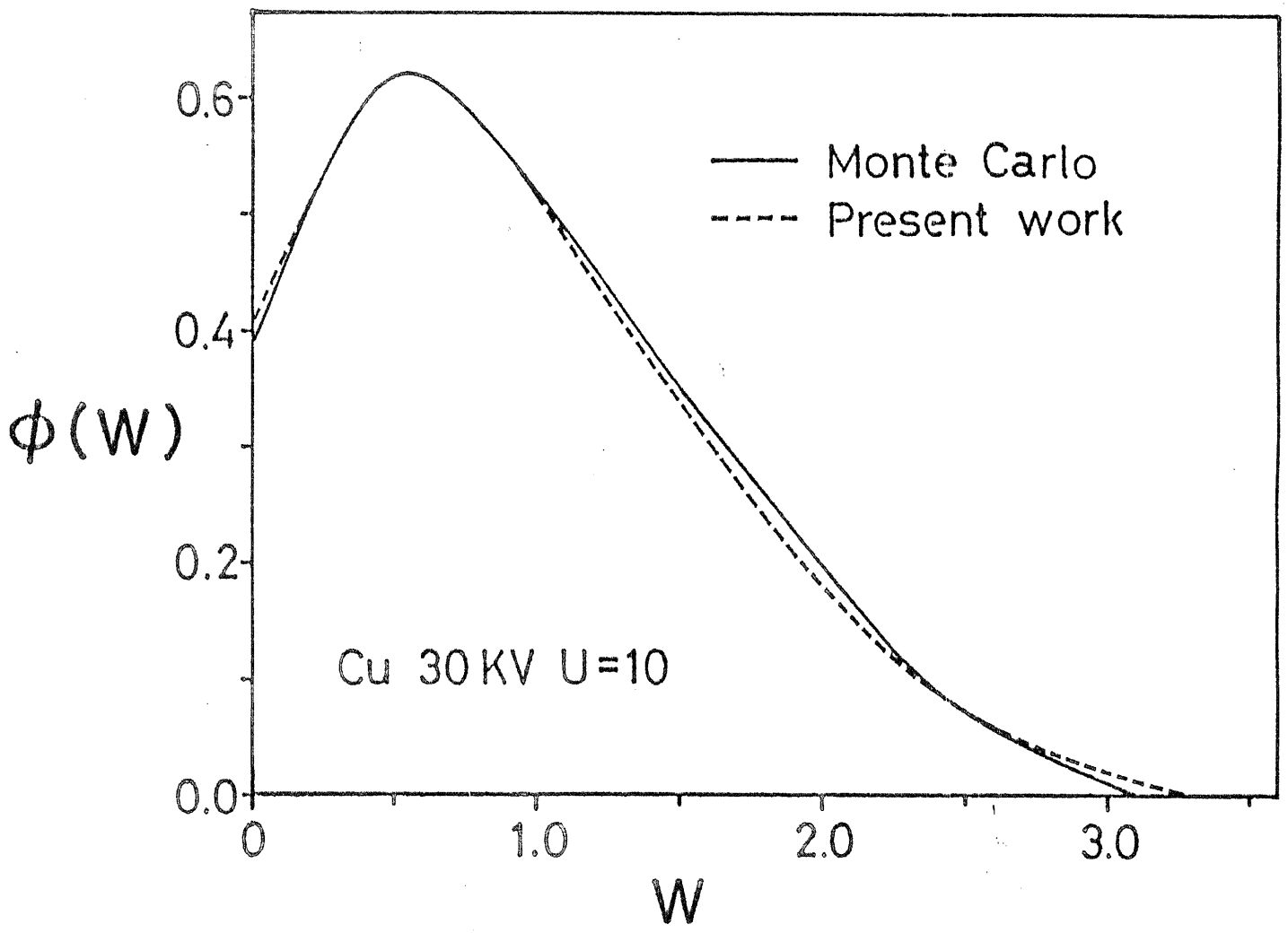

Fig. 3-5. Normalized ionization distribution in a copper matrix for an overvoltage ratio U=10 ; ——— Monte Carlo, ----- proposed ionization distribution equation.

The absorption correction equation can be derived from the equation (2) as follows.

$$f(\chi) = A\{\exp(V^2)\cdot \mathrm{Erfc}(V) - B\cdot\exp(u^2)\cdot\mathrm{Erfc}(u)\}$$

where

$$A = (e^{c^2}\cdot (1 + \mathrm{Erf}(c) - B))^{-1}$$

$$B = 6.65 \times 10^{-2}$$

$$u = \frac{1}{6.46}\chi.\overline{\rho z}\quad V = \frac{\chi.\overline{\rho z}}{1.33} - c, c = 0.1995 \text{ and}$$

$$\mathrm{Erfc}(y) = 1 - \mathrm{Erf}(y) = 1 - \frac{2}{\sqrt{\pi}}\int_0^y e^{-t^2}\,dt$$

In order to compare this $f(\chi)$ and $f(\chi)_{obs}$, the $f(\chi)/f(\chi)_{obs}$ ratios versus $f(\chi)_{obs}$ are shown in Figs.3-6,7 at accelerating voltage 30 kV. The $f(\chi)_{obs}$ used were calculated from $\phi(\rho z)$ determined by the tracer method (Parobek, 1972) and by the Monte Carlo method (Bishop, 1974). Figs.3-6,3-7 shows the $f(\chi)/f(\chi)_{obs}$ ratios are affected by the mean atomic number of matrix, however, the $f(\chi)/f(\chi)_{obs}$ ratios in Fig 3-7 gave satisfactory results in a wide range ($1.0 \geq f(\chi)_{obs} \geq 0.05$).

However, Fig 3-6 shows the $f(\chi)/f(\chi)_{obs}$ ratios do not coincide with 1.0, and this may be subject to the contribution from fluorescence effect on $\phi(\rho z)$ data

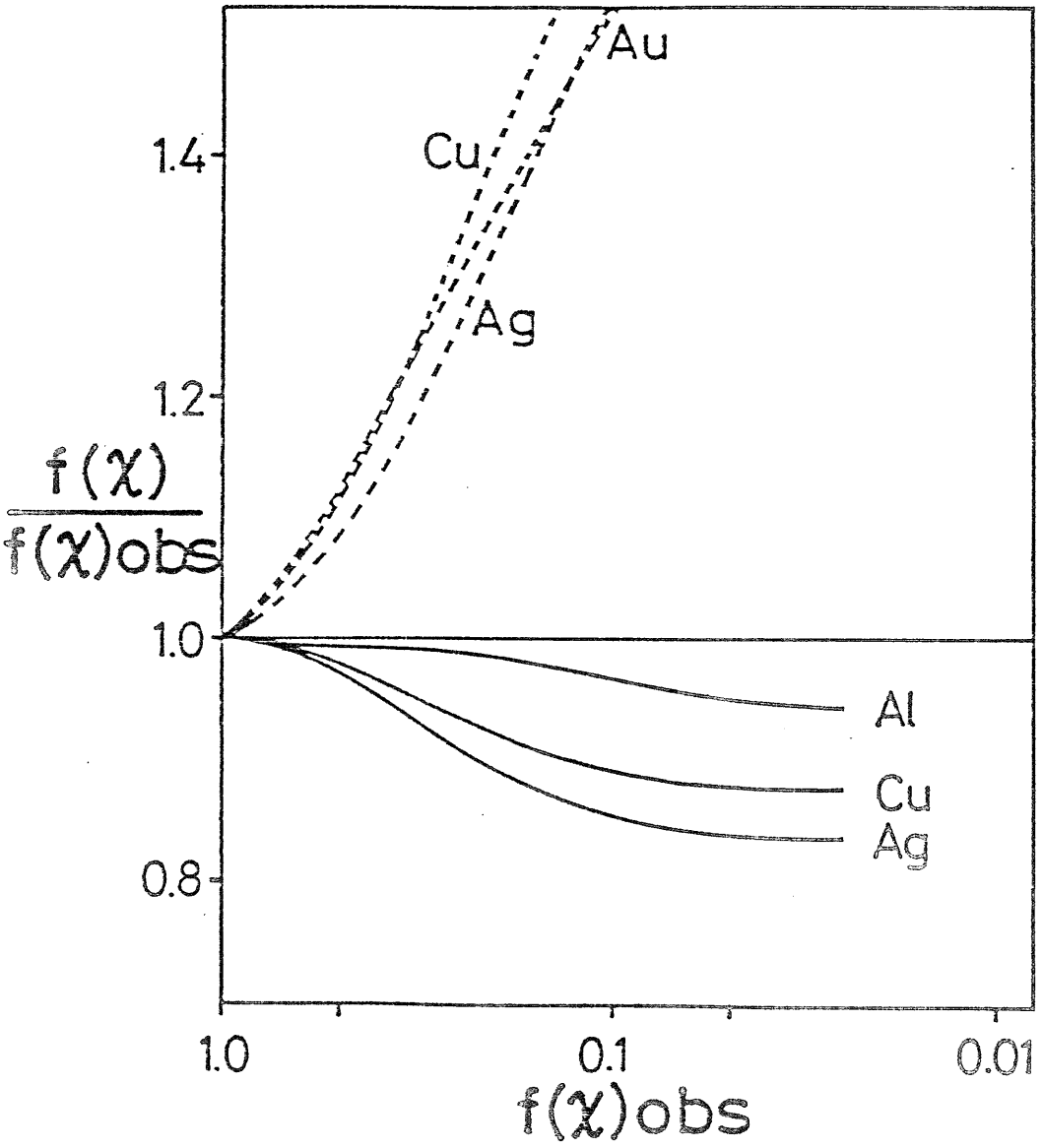

Fig. 3-6. Ratio of $f(\chi)/f(\chi)_{obs}$ using experimental ionization distribution for 30 kV (Bi tracer)

——— proposed absorption correction (II) ,

----- Simple Philibert equation.

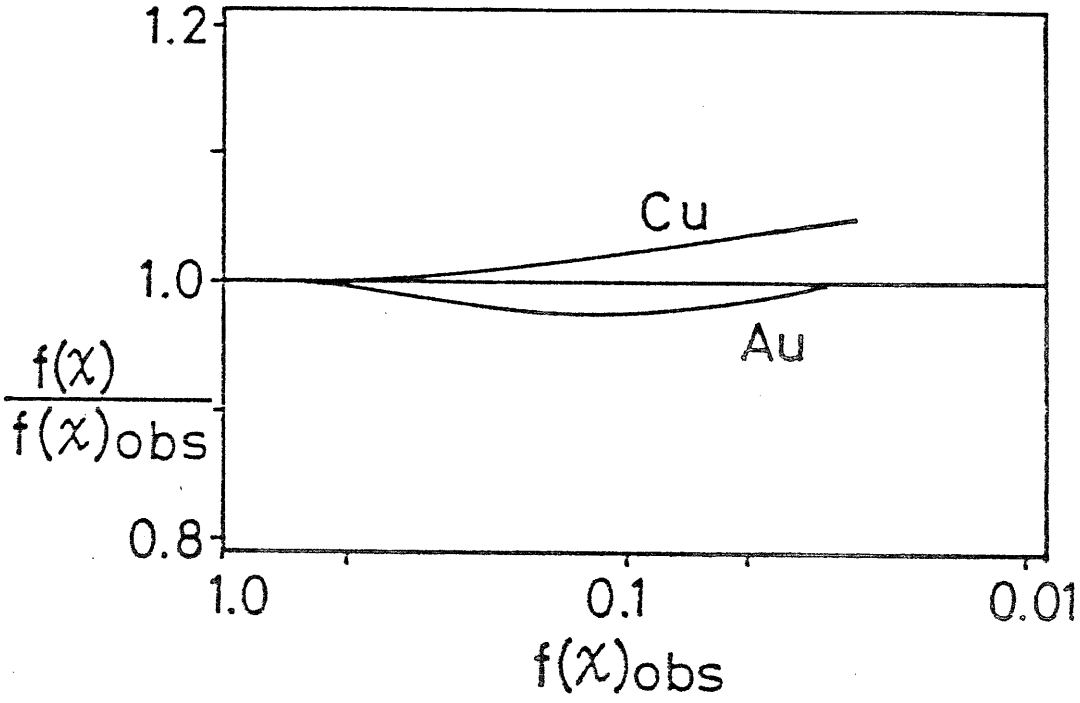

Fig. 3-7. Ratio of $f(\chi)/f(\chi)_{obs}$ using ionization distribution determined by Monte Carlo method for 30 kV and U=10. ——— proposed absorption correction (II).

determined by the tracer method. This $f(\chi)$ equation is very sensitive to the mean depth as the equation is shown by (4), and the correction for fluorescence effect is necessary because the mean depth of ionization is strongly affected by the fluorescence effect. Casting and Descamps (1954) pointed out that the contribution from the fluorescence effect was assumed to be constant down to depth of 1.2 mg/cm^2, and at depths greater than this directly produced ionization was assumed to be negligible.

The curves of $f(\chi)/f(\chi)_{obs}$ ratios curves $f(\chi)_{obs}$ which are calculated from experimental $\phi(\rho z)$ corrected for fluorescence effect are shown in Fig. 3-8, and this figure shows the proposed new $f(\chi)$ equation gave satisfactory value against the $f(\chi)_{obs}$ in a wide range ($1.0 \geq f(\chi) \geq 0.05$).

In general low $f(\chi)$ value are only encountered for relatively soft radiation where $U > 10$. Therefore, this equation might be expected to give good correction value in light element analysis because Fig.3-8 shows the $f(\chi)$ value is in close agreement with $f(\chi)_{obs}$ value even in lower range.

3.2.1 Examination of Mean Depth of Ionization

Mean depth of ionization $\overline{\rho z}$ is expected to obey the simple scaling law and will be a function of beam energy,

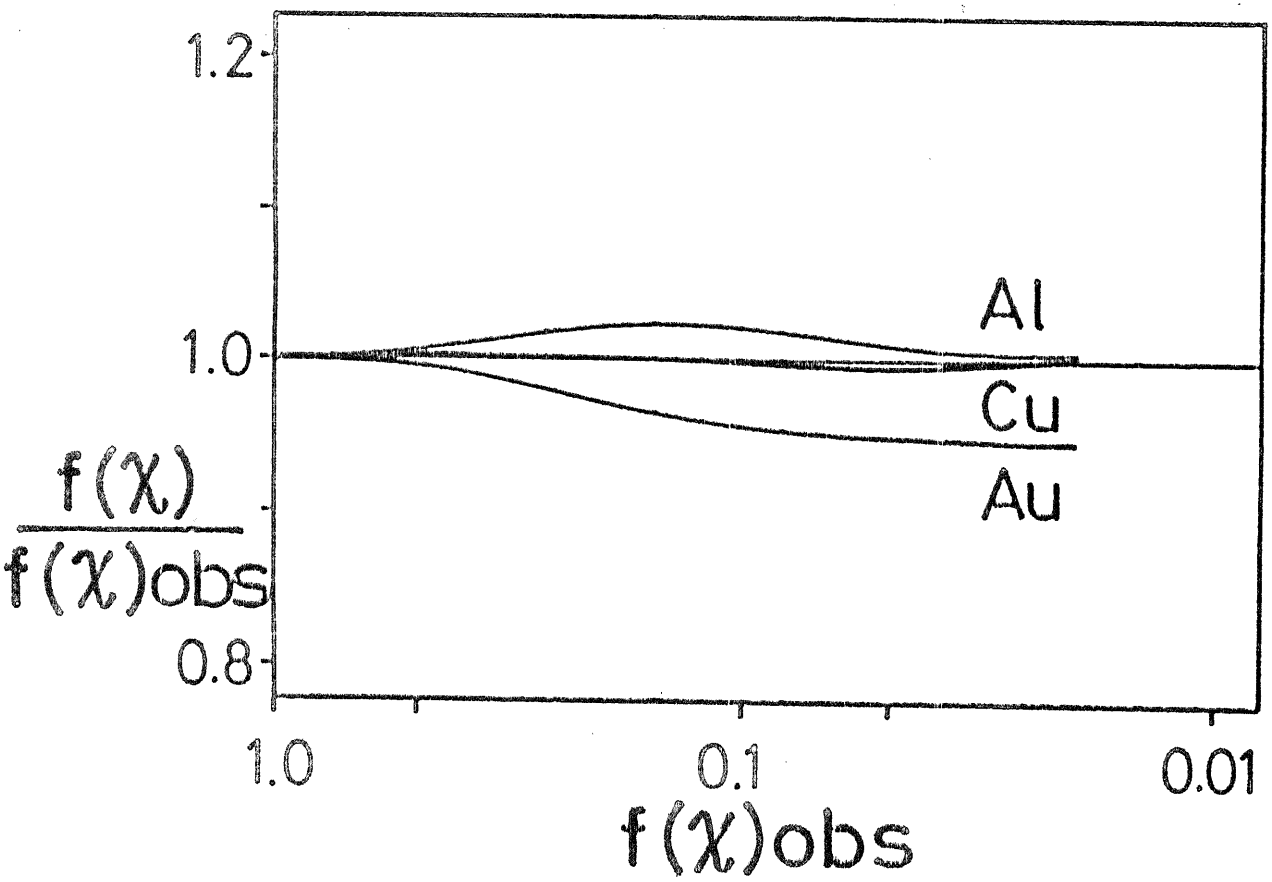

Fig. 3-8. Ratio of $f(\chi)/f(\chi)_{obs}$ using experimental ionization distribution corrected for fluorescence effect. ——— proposed absorption correction (II).

critical excitation potential, and the mean atomic number of the target. The $\phi(\rho z)$ equation proposed by Philibert (1963) is described as

$$\phi(\rho z)=\xi \exp(-\sigma\rho z) - (\xi- \phi(0))\exp(-(1+1/h)\sigma\rho z),$$

where ξ represents the scattering function at a depth greater than the depth of complete diffusion and equals to 4 theoretically, σ is the Lenard coefficient, and h represents the variation with atomic number. Using this equation, the mean depth $\overline{\rho z}$ is expressed as

$$\overline{\rho z} = \frac{1}{\sigma} \frac{q^2 - p}{q^2 - pq}$$

where

$$p = 1 - \frac{\phi(0)}{\xi} \quad \text{and} \quad q = \frac{h + 1}{h}$$

Various equations have been proposed for σ, and many equations of $\overline{\rho z}$ can be lead by them. The representative $\overline{\rho z}$ equations are listed as follows.

i) simple Philibert model

a) $$\overline{\rho z} = \frac{2h + 1}{1 + h} \cdot \frac{E_0^{1.65} - E_c^{1.65}}{4.5 \times 10^5}$$

where $h = 1.2\ A/Z^2$ and the constant of 1.65 and 4.5×10^5 were determined by Heinrich (1967).

b) $$\overline{\rho z} = \frac{2h + 1}{1 + h} \quad \frac{E_0^{1.5} - E_c^{1.5}}{2.39 \times 10^5} ,$$

where $h = 1.2\ A/Z^2$ and the constants 1.5 and 2.39×10^5 were determined by Duncumb-Shields (1966).

c) $$\overline{\rho z} = \frac{2h + 1}{1 + h} \quad \frac{E_0^{1.86} - E_c^{1.86}}{6.8 \times 10^5} ,$$

where $h = 0.85\ A/Z^2$, and the constants 1.86, 6.8×10^5, and 0.85 were determind Love et al. (1975).

ii) full Philibert model

d) $$\overline{\rho z} = \frac{1}{\sigma} \quad \frac{q^2 - p}{q^2 - pq} ,$$

where $h = 4.5\ A/Z^2$, $\sigma = \frac{2.54 \times 10^5}{E_0^{1.5} - E_c^{1.3}}$ and σ was determined by Duncumb-Merford (1966).

e) $$\overline{\rho z} = \frac{1}{\sigma} \quad \frac{q^2 - p}{q^2 - pq} ,$$

where $h = 1.5\ A/Z^2$, $\sigma = 9.5 \times 10^5/(E_0^2 - E_c^2)$ and σ was determined by Love et al. (1975).

In order to establish the accurate equation $\overline{\rho z}$ for the proposed $f(\chi)$, above $\overline{\rho z}$ equations which were used in the proposed absorption correction, were applied to the analysis of binary alloy systems together with Pool-Thomas (1962) atomic number correction, and the micronalysis data (150) were quoted in Pool's data (1968). No fluorescence correction was applied because this correction may play little part in this investigation. Calculated results are listed in Table 3-2. This table shows that the results obtained by applying Heinrich's mean depth equation gives the best results. The new absorption correction equation gives 5.5 % RMS error. That is, in heavier element analysis ($Z > 12$), much better than the result obtained by commonly used Philibert correction (6.2% RMS error).

4. Conclusion

The two new absorption corrections, one, associated with the Gaussian ionization distribution (I) and the other, associated with the new ionization distribution (II) were established.

The first (I) is expressed as

$$f(\chi) = A \exp(u^2) \cdot \mathrm{Erfc}(u) \qquad \text{(I)}$$

where, $A = \exp(-b^2)/(1 + \mathrm{Erf}(b))$, $u = q\chi - b$, $b = \frac{4}{15}$

Table 3-2 RMS errors of microanalysis results on binary alloy systems (150 measurements) using proposed absorption correction associated with various mean depth of ionization equations.

Mean depth of ionization	RMS error (%)
Love-Scott*	6.10
Duncumb-Shield*	6.24
Heinrich*	5.46
Duncumb-Merford**	7.63
Love-Scott**	9.88

* Simple Philibert model

** Full Philibert model

Atomic number correction : Pool-Thomas equation

$$\mathrm{Erfc}(y) = 1 - \mathrm{Erf}(y) = 1 - \frac{2}{\sqrt{\pi}} \int_0^y \exp(-t^2)\,dt$$

and $q = 1.158 \times 10^{-6}(E_0^{1.59} - E_c^{1.33})A/Z^{1.1}$ g/cm^2

or $q = 8.6 \times 10^{-7} E_0^{1.53}(1 - (E_c/E_0)^{3.16})A/Z$ g/cm^2 .

The second one (II) was obtained from the new $\phi(w)$ function, $\phi(w) = 0.644\ e^{-0.665^2(w - 0.3)^2} - 0.2e^{-3.23^2 w^2}$, and is expressed as

$$f(\chi) = A\{\exp(v^2)\cdot\mathrm{Erfc}(v) - B\exp(u^2)\mathrm{Erfc}(u)\} \quad \text{(II)}$$

where

$$A = (\exp(c^2)\cdot(1 - \mathrm{Erf}(c) - B)^{-1}$$

$$B = 6.65 \times 10^{-2}$$

$$u = 1/6.46\ \chi\cdot\overline{\rho z}\ ,\quad v = \frac{\chi\overline{\rho z}}{1.33} - c,\quad c = 0.1995$$

and

$$\overline{\rho z} = \frac{2h + 1}{1 + h}\ \frac{E_0^{1.65} - E_c^{1.65}}{4.5 \times 10^5}\ .$$

These equations, when combined with Pool-Thomas atomic number correction, give much better results (RMS error: 5.5% (I), 5.7% (II)) than those obtained by commonly used Philibert absorption corrections (simple Philibert : 6.2%, full Philibert : 8.3%) on binary alloy systems (150 measurements).

In wide range, $f(\chi)$ values predicted by the proposed equations are coincident with those of $f(\chi)_{obs}$ calculated from $\phi(\rho z)_{obs}$ which were determined by the Monte Carlo method or by the tracer method. The proposed equations may be expected to give accurate corrected results in light element analysis.

Chapter 4. Evaluation of the New Absorption Corrections on Light Element Analysis

1. Introduction

The author proposed two absorption corrections in chapter 3. And these equations gave good results of analysis in binary alloy systems, and were expected to give good results in light elements analysis because $f(\chi)$ values predicted by the proposed equations are coincident with those of $f(\chi)_{obs}$ calculated from the experimental $\phi(\rho z)$ in wide range.

The proposed two absorption corrections are evaluated using many microanalysis data of oxygen in inorganic compounds in this chapter. Results are compared with those obtained commonly used simple Philibert and full Philibert absorption correction.

2. Correction Procedures

2.1. Atomic Number Correction

The atomic number correction is treated separately considering the stopping power factor S and backscattering factor R, and is written as

$$\frac{I_{sp}}{I_{std}} = \frac{C_{sp} \cdot R_{sp} \cdot (1/S_{sp})}{C_{std} \cdot R_{std} \cdot (1/S_{std})}$$

The Duncumb-Reed (1968) or Philibert-Tixier (1968) correction are commonly used for factor S, and these two corrections gave the same order results (Love et al. 1975). As the former equation is rather simpler than the latter, the Duncumb-Reed atomic number correction was used in this investigation.

The correction is described as follows.

stoppting power S : $S = \Sigma\, C_i Z_i / A_i \cdot \ln(1.166\bar{E}/J_i)$, where $\bar{E} = (E+E_c)/2$ and J_i is mean ionization potential of element i, and backscattering R :

$$R = 1 - \eta_x = \Sigma(1 - \eta_{xi})$$

where

$$\eta_{xi} = \frac{\int_{w_c}^{1} \eta(w)\, Q/s\, dw}{\int_{E_c}^{E_o} Q/s\, dE} = \frac{\int_{w_c}^{1} \eta(w) \ln(w)\, dw}{\int_{w_c}^{1} \ln(w)\, dw}$$

Ans η is called"electron backscattering coefficient". Many equations have been proposed for the mean ionization potential J, and J = 13.5×Z(eV) was used in this study because the ionization potential of hydrogen is 13.6 eV and 13.5 eV is in close agreement with Duncumb et al's J/Z data (1968) for high atomic number elements. The following equations were used for the calculation of the backscattering factor R.

$$R = 1 - \eta(I(U_0) + \eta G(U_0))^{1.67}$$

where, $I(U_0) = A_1 \ln U_0 + A_2(\ln U_0)^2 + A_3(\ln U_0)^3 + A_4(\ln U_0)^4$

and

$$G(U_0) = \frac{1}{U_0}(B_1 \ln U_0 + B_2(\ln U_0)^2 + B_3(\ln U_0)^3 + B_4(\ln U_0)^4)$$

where $U_0 = E_0/E_c$.

The constants A_i and B_i were determined by Love et al. (1978).

2.2. Absorption Correction

The proposed two absorption corrections are described as follows.

(I) $f(\chi) = A \exp(u^2)\mathrm{Erfc}(u)$

where

$$u = q\chi - b.$$

(II) $f(\chi) = A(\exp(v^2)\mathrm{Erfc}(v) - B \cdot \exp(w^2)\mathrm{Erfc}(w))$

where

$$v = \chi\overline{\rho z}/1.33 - c \text{ and } w = \chi\overline{\rho z}/6.46.$$

And $\overline{\rho z}$ (mean depth of ionization) given by Heinrich(1967) was used in this correction. q in the equation (I) was already discussed in chapter 3. The simple Philibert and full Philibert absorption correction were compared with above equation.

These are described as ;

Simple Philibert equation :

$$f(\chi) = (1+h)/(1+ \chi/\sigma)/(1+h(1+ \chi/\sigma))$$

where $h = 0.85\ A/Z^2$ and $\sigma = 6.8 \times 10^{-5}/(E_0^{1.86} - E_c^{1.86})$.

Full Philibert equation :

$$f(\chi) = \frac{1 + \dfrac{\phi(0)\,h}{4+\phi(0)\,h}\ \dfrac{\chi}{\sigma}}{(1+\chi/\sigma)\left(1+\dfrac{h}{1+h}\ \dfrac{\chi}{\sigma}\right)}$$

where $\phi(0) = 1 + 2.8(1-0.9E_0/E_c)$, $h = 1.5A/Z^2$ and $\sigma = 9.5 \times 10^5/(E_0^2 - E_c^2)$.

Lenard coeffcient σ and mean atomic number variation h determined by Love et al. (1975) were used because they gave better results than others in the analysis of binary alloy systems. No fluorescence correction is applied because the contribution is negligible in the analysis of light elements.

Then, theoretical intensity ratio k' can be described as

$$k' = \frac{C_{sp} \cdot f(\chi)_{sp} \cdot R_{sp} \cdot S_{std}}{C_{std} \cdot f(\chi)_{std} \cdot R_{std} \cdot S_{sp}}$$

3. Results and Discussion

The measurement was carried out on the following samples; silicates, sulfates, doulble oxides of lanthanoid and niobium and binary oxides.

1) silicates : SiO_2, $CaSiO_3$, $NaAlSi_3O_8$, $KAlSi_3O_8$

2) sulfates : $CaSO_4$, $SrSO_4$, $BaSO_4$, $PbSO_4$

3) double oxides of lanthanoid and niobium :

$LaNbO_4$, $TbNbO_4$, $ErNbO_4$, $EuNbO_4$, $GdNbO_4$

4) binary oxides : Fe_2O_3, MgO, TiO_2, Cr_2O_3

Measured data of oxygen in those samples have already shown in chapter 2 (Table 2-2,5,7,9). Data for $MgAl_2O_4$, $FeTi_2O_5$, $NiTiO_3$, $PbMoO_4$ and $CaZrO_3$ quoted from Love et al.'s work (1974b) are also used for this investigation. The accelerating voltage range were from 5 to 30 kV.

The 160 measurements data of oxygen have been plotted as c /k in a histogram (Fig.4-1) in order to indicate the order of magnitude of the correction required ; c is concentration ratio and k the measured intensity ratio (standard : Al_2O_3). Microanalysis data were corrected applying each absorption correction together with Duncumb-Reed (1968) atomic number correction. The mass absorption coefficients used were those given by Love et al. (1974b) ($8 \leq Z < 22$, $Z = 80$) and Henke et al. (1974) ($22 \leq Z \leq 79$).

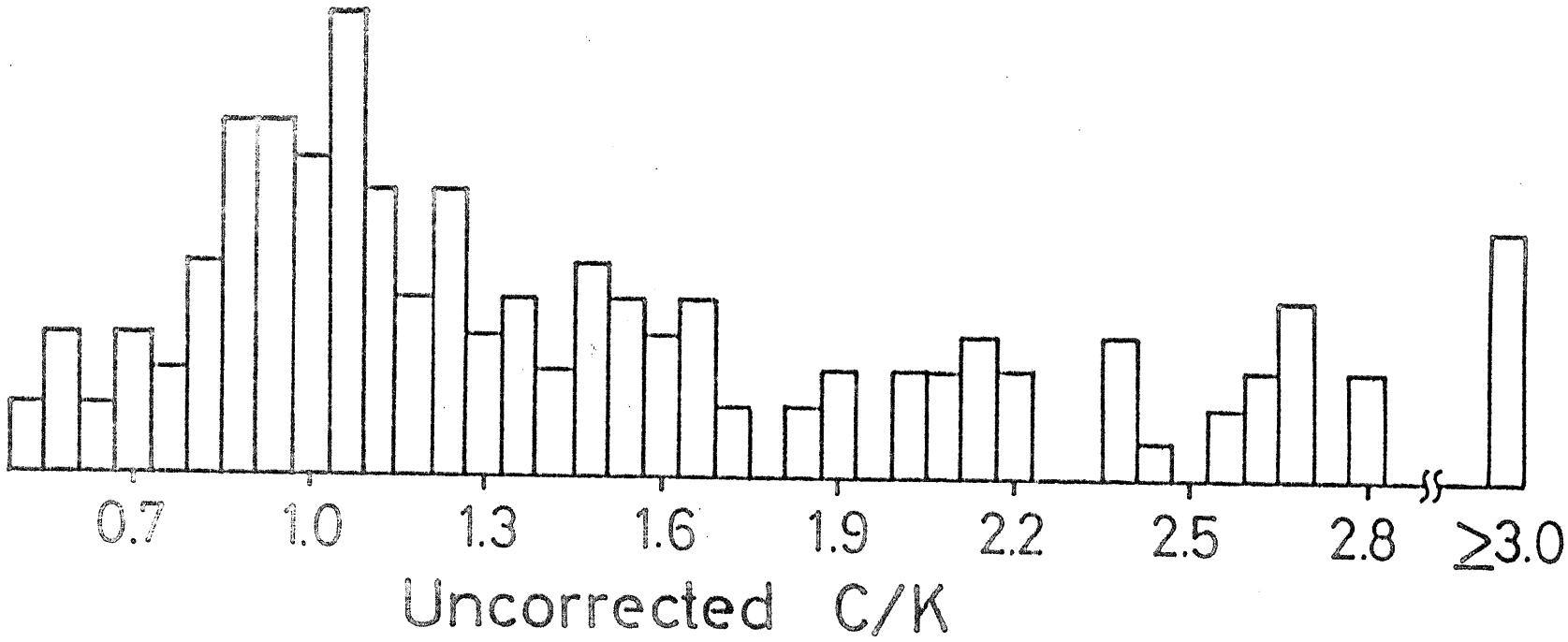

Fig. 4-1. Histogram of uncorrected microanalysis data of oxygen (160 measurements). C is the relative concentration and k is measured intensity ratio of oxygen using aluminium oxide as a standard.

The following equation which gave better RMS error (mean : 5.64%) than that of others (7.59%) for the oxygen analysis was chosen.

$$q = 1.158 \times 10^{-6}(E_0^{1.59} - E_c^{1.33})A/Z^{1.1} \quad (g/cm^2)$$

The new absorption correction (I) and (II) gave better results than those given by commonly used Philibert correction as shown in Table 4-1. Especially the new correction (II) gave very good results (within 5% RMS error). Microanalysis data obtained by applying various absorption corrections together with the Duncumb-Reed atomic number correction (1968) are shown in Fig 4-2 as the form of histograms of k'/k. This figure clearly shows either of absorption correction proposed in this thesis is better than commonly used Philibert models. RMS error of corrected analytical results obtained by the proposed correction (I) and (II), simple Philibert and full Philibert absorption correction are compared in Table 4-2.

This table indicates over 60% of the data corrected by proposed equation (I) or (II) lay within 5% of the true value. This result is as good as that of ordinary element analysis, ie. Si, Al, Fe and other major components in silicate minerals, by electron probe

Table 4-1 RMS error of k'/k in oxygen analysis

Absorption correction	RMS error (%)				
	Silicate	Sulfate	$LnNbO_4$*	Binary oxide	Ternary oxide
Simple Philibert	6.01	11.8	9.01	11.5	8.97
Full Philibert	5.22	14.8	5.02	9.86	8.30
Proposed equation (I)**	5.29	7.73	4.11	5.88	5.52
(II)	3.46	6.74	4.12	4.67	6.06

Atomic number correction : Duncumb-Reed equation

Standard for oxygen : aluminium oxide

* Double oxide of lanthanoid and niobium

** $q = 1.158\times10^{-6}(E_o^{1.59}-E_c^{1.33})A/Z^{1.1}$ (cm^2/g)

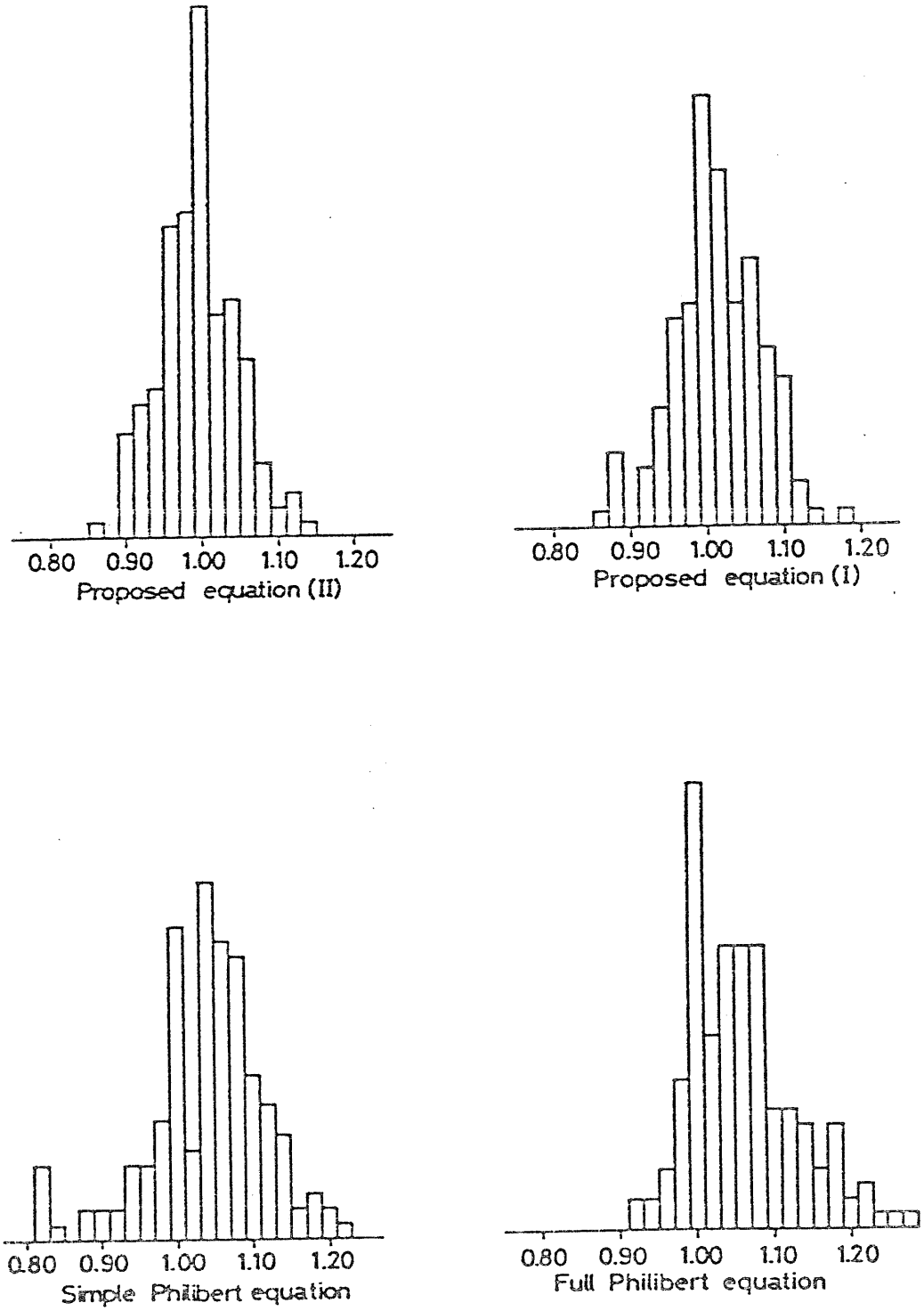

Fig. 4-2. Histograms of corrected microanalysis results k'/k using various absorption correction together with Duncumb-Reed atomic number correction. The standard for oxygen is aluminium oxide.

Table 4-2 Accuracy of microanalysis results of oxygen (160 measurements) using various absorption corrections

Absorption correction	RMS error (%)	% of results within 3% of true concentration	% of results within 5% of true concentration
Simple Philibert	9.55	21.9	40.0
full Philibert	8.52	33.1	47.5
Proposed equation (I)	5.64	42.5	60.6
(II)	4.98	49.4	68.8

Atomic number correction : Duncumb-Reed equation

microanalyzer. Therefore both absorption correction (I) and (II) can be applied to the practical analysis for light elements.

4. Conclusion

Proposed two absorption corrections were examined on 160 microanalysis data of oxygen in inorganic compounds. The following two absorption corrections gave greater accuracy than that of the Philibert absorption correction models. Proposed absorption corrections are written as

(I) $f(\chi) = A \exp(u) \cdot \mathrm{Erfc}(u)$

where $u = q\chi - b, \quad b = 5/14,$

$$q = 1.158 \times 10^{-6}(E_0^{1.59} - E_c^{1.33})A/Z^{1.1}.$$

$$f(\chi) = A\,(\exp(v^2) \cdot \mathrm{Erfc}(v) - \exp(w^2) \cdot \mathrm{Erfc}(w))$$

where

$$v = \chi\overline{\rho z}/1.33 - c, \quad c = 0.1995,$$

$$w = \chi\overline{\rho z}/6.46, \quad \overline{\rho z} = \frac{(E_0^{1.65} - E_c^{1.65})}{4.5 \times 10^5}$$

The RMS errors for oxygen analyses obtained using above equations were 5.6% and 5.0% respectively, and those values were superior to that obtained by the simple Philibert or by the full Philibert absorption correction (simple Philibert : 9.8%, full Philibert : 8.5%). Both new corrections could be applied to the practical analysis

of light elements because the magnitude of RMS error for oxygen analysis was as smsll as that of ordinary element analysis by electron microprobe.

Chapter 5. Quantitative Analysis of Hydrous Minerals

1. Introduction

There are many minerals which contain large quantity of water like zeolites and clay minerals. The analyses of these samples by electron probe microanalyzer have been a difficult problem because there is no suitable method to determine the water content in the analytical area on electron microprobe. If electron microprobe analysis of these samples were carried cut without the determination of water, the results of analysis might contain a large error caused by the correction calculation. Therefore it is very important to estimate the content of water for the analysis of these hydrous minerals.

The author carried out the determination of several zeolites and muscovite using OK_{α} line to estimate the total oxygen content in electron bombardment area. The content of water or hydroxyl group in these samples were determined by deducing the oxygen content combined with metals stoichiometrically from the total oxygen content.

2. Experimental

The EPMA system used consists of a JEOL JXA-50A electron probe microanalyzer and a ACPS-XR control

system designed by ELIONIX. The measurement conditions are represented in Table 5-1 in detail. The samples analyzed were muscovite, heulandite, laumontite, chabazite, analcime and yugawaralite. The standard specimens and analyzing crystals for each element are shown in Table 5-2.

3. Correction Procedures

The correction method used for the quantitative analysis of muscovite and several zeolites consist of the Duncumb-Reed atomic number correction, the proposed absorption correction (II) and the Reed fluorescence correction. The content of element i could be obtained from the measurement intensity ratio K_i according to the following equation.

$$K = \frac{C_i}{C_{i,std}} \cdot \frac{R_i}{R_{i,std}} \cdot \frac{1/S_i}{1/S_{i,std}} \cdot \frac{f(\chi)_i}{f(\chi)_{i,std}} \cdot \frac{(1+\gamma_i)}{(1+\gamma_i)_{std}} ,$$

where, the atomic number (R,S) and absorption correction ($f(\chi)$) are same as already described in chapter 4. The fluorescence correction is represented as the term $(1+\gamma)$, and γ can be written as

Table 5-1. Analytical conditions for determination of hydrous minerals

Acclerating voltage	: 15 kV
Beam current	: 0.013 μA on Faraday cage
PHA condition (for oxygen analysis)	
Lower level	: 1.0 V
Window	: 2.0 V
Gain	: 32×6
Discriminator mode	: diff

Table 5-2 The standard specimens and analyzing crystals for muscovite and zeolite analysis

Element	Standard	Analyzing crystal
O	Al_2O_3	STE
Na	$NaAlSi_3O_8$	RAP
Mg	MgO	RAP
Al	Al_2O_3	RAP
Si	SiO_2	RAP
K	$KAlSi_3O_8$	PET
Ca	$CaSiO_3$	PET
Fe	Fe_2O_3	LiF

$$\gamma_i = C_j J(i) D \frac{(\mu/\rho)_j^i}{(\mu/\rho)_j^{ij}} \{g(x) + g(y)\}$$

where

$$g(Z) = \frac{\ln(1+Z)}{Z}, \quad y = \sigma/(\mu/\rho)_i^{ij}$$

$$x = \{(\mu/\rho)_i^{ij}/ (\mu/\rho)_j^{ij}\} \operatorname{cosec} \theta ,$$

and

$$D = \left(\frac{U_0^j - 1}{U_0^i - 1} \right)^{1.67} .$$

4. Results and Discussion

4.1. Muscovite

Muscovite has hydroxyl group which is quite resistant to the electron bombardment. The determination of OH content in muscovite was carried out by electron microprobe in order to examine the ability to determine the oxygen content by ZAF correction, which includes the proposed absorption correction in this thesis. The content of oxygen in hydroxyl group was decided deducing the oxygen content combined with metals stoichiometrically from the total oxygen content.

The results of analyses of muscovite from Ishikawa, Fukushima Prof. and Zambei, Zambia are shown in Table 5-3 and 5-4 respectively. The following empirical formulas on the basis of total oxygen atoms as 24 were

Table 5-3. Microprobe analysis of muscovite (A); (Zambei, Zambia)

Element	K-val*(wt%)	Concentration (wt%)	No. of atoms (24 oxygens)
O	34.11	47.33	(24)
Na	0.35	0.39	0.14
Mg	0.42	0.50	0.17
Al	15.64	16.92	5.09
Si	17.38	21.06	6.08
K	10.30	10.25	2.13
Fe	2.73	3.08	0.45
total	80.93	99.53	14.06

* Measured relative intensity

Table 5-4 Microprobe analysis of muscovite (B); (Ishikawa, Fukushima)

Element	K-val*(wt%)	Concentration (wt%)	No. of atoms (24 oxygens)
O	35.22	47.78	(24)
Na	0.44	0.48	0.17
Mg	—	—	—
Al	17.38	18.61	5.54
Si	16.89	20.70	5.92
K	9.40	9.37	1.93
Fe	2.40	2.70	0.39
total	81.73	99.64	13.95

* Measured relative intensity

obtained from the results of analyses given in these tables.

A: muscovite (Zambei, Zambia)

$$(K_{2.13}, Na_{0.14})_{2.27}(Al_{3.17}, Fe_{0.45}, Mg_{0.17})_{3.79}(Al_{1.92}Si_{6.08})_8O_{19.55}(OH)_{4.45}$$

B: (Ishikawa, Fukushima Pref.)

$$(K_{1.91}, Na_{0.19})_{2.10}(Al_{3.46}, Fe_{0.39})_{3.85}(Al_{2.08}, Si_{5.92})_8O_{19.57}(OH)_{4.43}$$

The ignition losses of thses two muscovites were determined in order to compare with the calculated content of water obtined from the above two empirical formulas.

The losses on ignition was 5.30% on sample A and 4.90% on sample B, and agreed with those obtained from empirical formulas (A : 4.93%, B : 4.95%). The content of OH are also in agreement with the theoretical formula of muscovite. These results imply the reliability of the proposed method.

4.2. Zeolite

The examination of the characteristics of OK_α line of the typical anhydrous oxide SiO_2 and typical hydrous silicalte, zeolite, had been carried out in

order to find the difference between them. No clear change caused by the water was found on the shape or shift of OK_α line. Therefore, the peak intensity of OK_α line might give the information of total oxygen content in zeolite samples. And the analyses of several zeolites, ie. heulandite, laumontite, chabazite, analcime and yugawaralite, were carried out. The water content of them were determined deducing the oxygen content combined with metals stoichometrically from the total oxygen content. The results of analyses are shown in Tables 5-5(heulandite), 5-6(laumontite), 5-7 (chabazite), 5-8(analcime) and 5-9(yugawaralite), and the following empirical formulas for these zeolites were obtained on the bases of total atoms of Si and Al as 9.0 in heulandite, 6.0 in laumontite and chabazite , 8.0 in yugawaralite and 3.0 in analcime.

Heulandite :

$$(Ca_{0.27},K_{0.17},Na_{0.46})_{0.90}(Al_{1.91},Si_{7.09})_9O_{17.63}\cdot 4.81\ H_2O$$

Lanmontite :

$$(Ca_{0.83},K_{0.03},Na_{0.08})_{0.94}(Al_{1.76},Si_{4.24})_6O_{12.01}\cdot 4.60\ H_2O$$

Chabazite :

$$(Ca_{0.84},K_{0.04},Na_{0.03})_{0.91}(Al_{1.80},Si_{4.20})_6O_{11.95}\cdot 5.79\ H_2O$$

Table 5-5. Microprobe analysis of heulandite

Element	K-val(wt%)*	Concentaration (wt%)	No. of atoms (Al+Si=9)
O	48.72	56.55	22.44
Na	1.54	1.68	0.46
Al	7.54	8.13	1.91
Si	28.02	31.36	7.09
K	1.01	1.03	0.17
Ca	1.56	1.69	0.27
total	88.39	100.44	

* Measured relative intensity

Table 5-6. Microprobe analysis of laumontite

Element	K-val (wt%)*	Concentration (wt%)	No. of atoms (Al+Si=6)
O	39.03	56.99	16.60
Na	0.37	0.40	0.08
Mg	0.02	0.02	
Al	9.61	10.19	1.76
Si	22.27	25.55	4.24
K	0.24	0.24	0.03
Ca	6.68	7.16	0.83
total	78.22	100.55	

* Measured relative intensity

Table 5-7. Microprobe analysis of chabazite

Element	K-val(wt%)*	Concentration (wt%)	No. of atoms (Si+Al=6)
O	41.30	58.73	17.76
Na	0.11	0.12	0.03
Al	9.38	10.03	1.80
Si	21.22	24.39	4.20
K	0.29	0.29	0.04
Ca	6.51	6.98	0.84
total	78.71	100.54	

* Measured relative intensity

Table 5-8. Microprobe analysis of analcime

Element	K-val(%)*	Concentration (wt%)	No. of atoms (Al+Si=3)
O	53.41	51.97	7.06
Na	8.44	9.00	0.85
Al	9.46	10.90	0.88
Si	23.07	27.41	2.12
K	0.05	0.05	-
total	94.43	99.33	

* Measured relative intensity

Table 5-9. Microprobe analysis of yugawaralite

Element	K-val(%)*	Concentration (wt%)	No. of atoms (Al+Si=8)
O	37.88	55.38	20.91
Al	8.37	8.77	1.96
Si	25.03	28.07	6.04
K	0.07	0.07	-
Ca	6.24	6.70	1.01
total	77.59	98.99	

* Measured relative intensity

Analcime :

$$Na_{0.85}(Al_{0.88},Si_{2.12})_3O_{5.99}\cdot 1.08\ H_2O$$

Yugawaralite :

$$Ca_{1.01}(Al_{1.96},Si_{6.04})_8O_{16.03}\cdot 4.88\ H_2O$$

The ratios of A to B, where A represents Ca, Na, K and B does Al, Si in the empirical formulas obtined for these zeolites agree with those of theoretical ones, indicating that the proposed correction method give good results of analyses for ordinary element in hydrous samples like zeolites.

The content of water in zeolite samples were calculated from the above empirical formulas, and are shown in Table 5-10 together with the water content determined by the thermo-gravimetric analysis. Although the results of H_2O analysis by this proposed method are affected by the errors of analysis of other elements, may be applicable to the practical analysis of zeolites.

On the other hand, the water content obtained by T.G. method represent the average quantity of water in the samples, and do not give the water content of micro

Table 5-10. Determination of water content in zeolite by electron probe microanalyzer

Sample	Water content (wt%) EPMA	T.G.*
Heulandite	13.4	13.7
Laumontite	8.9	9.7
Chabazite	20.9	20.6
Analcime	15.0	14.0
Yugawaralite	17.3	17.6

* Thermo-gravimetric analysis

area like that obtained by the electron probe analysis. Taking these facts into consideration, the water content determined by proposed method are good agreement with T.G. method. The results of this method may represent the content of water in the electron bombardment area, and this proposed method could be applied to the determination of water content in μm order area in hydrous minerals.

5. Conclusion

The electron probe analysis of muscovite, which contains hydroxyl group, and zeolite, which contains water, were carried out using Ok_{α} line. The intensity of OK_{α} line gave the information of total oxygen content including the oxygen in OH and H_2O. The proposed method, to determine water content or hydroxyl group content by deducing the oxygen combined with metals stoichiometrically from the total oxygen content, was applied to the total analysis of muscovite and several zeolites, ie. heulandite, laumontite, chabazite, analcime and yugawaralite.

In the analysis of muscovite this method gave satisfactory results. The number of OH obtained by the proposed method is in good agreement with the number of OH in the ideal formula, and the water content determined from the the obtained empirical formula given by

this method are also in good agreement with the results given by ignition loss.

In the analysis of zeolite, this method also gave satisfactory results. The empirical foumulas calculated from the results obtained by this method are quite reliable, and the content of water obtained by this method agreed with the results of T.G. method within 10%. The method must give the content of water in electron bombardment area.

Chapter 6. Conclusion

In conclusion, the following facts were defined.

(1) The most suitable accelerating voltage for the practical analysis of oxygen in inorganic compounds is in the range $10 \leq E_0 \leq 15$ kV.

(2) The full Philibert absorption correction gave better results in the oxygen analysis than that of the simple Philibert or Yakowitz-Heinrich absorption correction because of the contribution of $\phi(0)$ term in the high accelerating voltage range.

(3) Even the full Philibert absorption correction, did not give satisfactory results to all measured accelerating voltage and samples. For example, the correction gave good results for silicates (5.2%) and double oxides of lanthanoid and (5.2%), but gave large RMS error for oxygen analysis in sulfates (14.8%), binary oxide (9.8%) and ternary oxide systems (8.3%). Therefore an improved absorption correction is required for the quantitative analysis of light elements.

(4) A new absorption correction is established based on the Gaussian ionization distribution, which was proposed by Wittry.

The correction is expressed as

$$f(\chi) = A \cdot \exp(u^2) \cdot \mathrm{Erfc}(u) \qquad (I)$$

where, $u = q\chi - b$, $b = 5/14$

and $q = 1.158 \times 10^{-6}(E_0^{1.59} - E_c^{1.33})A/Z^{1.1}$.

(5) A new normalized ionization distribution is established by the nonlinear least square curve fitting using the data of $\phi(w)$, which was determined by the Monte Carlo method, in a Cu target at 30 kV and U = 10. The new normalized ionization distribution proposed is written as

$$\phi(w) = 0.664 \cdot \exp(-0.665^2(w-0.3)^2) - 0.2 \cdot \exp(-3.23^2 w^2).$$

(6) A new absorption correction associated with the new normalized ionization distribution in (5) is obtained, and is expressed as

$$f(\chi) = A(\exp(v^2)\mathrm{Erfc}(v) - \exp(w^2)\mathrm{Erfc}(w)), \qquad (II)$$

where,

$V = \chi \cdot \overline{\rho z}/1.33 - C$, $C = 0.1995$

$w = \chi \cdot \overline{\rho z}/6.46$ and $\overline{\rho z} = (E_0^{1.65} - E_c^{1.65})/4.5 \times 10^5$.

(7) Proposed two absorption corrections were examined on 310 microanalysis data (light elemets : 160,

heavier elements ($Z \geq 12$) : 150). The proposed absorption correction gave greater accuracy than that of the Philibert correction models. The RMS errors of oxygen analysis obtained using proposed absorption corrections were 5.6% (equation I) and 5.0% (equation II) respectively, and that of the other elements analysis in binary alloy systems was 5.7% and 5.5% respectively. These values were superior than that of simple Philibert (heavier elements : 6.2%, oxygen :9.6%) or full Philibert absorption correction (heavier elements : 8.3%, oxygen : 8.5%). Therefore, both proposed new corrections could be applied to the practical analysis of light elements.

(8) The proposed absorption correction (II) was applied to the analyses of muscovite and several zeolites, which have OH or H_2O, together with Duncumb-Reed atomic number and Reed fluorescence correction. In order to determine the content of water or hydroxyl group in micro area, the following method is proposed because the intensity of OK_α line gives the information of total oxygen content.

H_2O (OH) (wt%) = O (wt%)$_{total}$ - ΣO_i,

where O_i represents the content of oxygen combined with stoichiometrically.

(9) This proposed method for determination of water or hydroxyl group content gave satisfactory results in the analysis of muscovite, heulandite, laumontite, chabazite, yugawaralite and analcime. The empirical formulas calculated from the results obtained by this method were quite reliable, and the content of water or hydroxyl group obtained agreed with the results of T.G. method. This method must give the content of water or hydroxyl group in electron bombardment area.

Acknowledgments

The author wishes to thank Prof. Kozo Nagashima for his continuing interest and encouragement for this investigation.

He is also grateful to Dr. Y. Sugitani, Dr. Y. Yano and Dr. I. Nakai for their helpful advices and discussions, and Mr. N. Nishida, Chemical Analysis Center of the University of Tsukuba, for useful suggestions for measurements by electron microprobe.

References

Andersen, C. A., and Wittry, D. B. (1968). J. Phys. D: Appl. Phys. 1, 529.

Bishop, H. E. (1974).ibid, 7, 2009.

Brown, J. D. and Parobek, L. (1972). "Proceedings of the Sixth International Conference on X-ray Optics and Microprobe Analysis", p163, University of Tokyo Press.

_____ ,(1975). X-ray Spectrometry, 5, 36.

_____ ,(1978). ibid, 7, 26.

Cosslet, V. E. and Thomas, R. N. (1966). Brit. J. Appl. Phys., 15, 1283.

Duncumb, P and Merford, D. A. (1966). "X-ray Optics and Microanalysis ", eds. R. Casting, P. Descampas and J. Philibert, p240, Herman, Paris.

Duncumb, P. and Reed, S. J. B. (1968). "Quantitative Electron Probe Microanalysis", ed. K. F. J. Heinrich, p133, NBS Special Publication.

Green, M and Cosslet, V. E. (1961). Proc. Phys. Soc., 78, 1206.

Heinrich, K. F. J. and Yakowitz, H. (1975). Anal. Chem., 47,2408.

Kyser, D. F. (1972). "Proceedings of the 6th International Conference on X-ray Optics and Microanalysis", eds. G. Shinoda, K. Kohra and T. Ichinokawa, p147, Toyo Press, Tokyo.

Love, G., Cox, M. G. C. and Scott, V. D. (1974a). J. Phys. D: Appl. Phys., 7, 2131.

_____ ,(1974b). ibid, 7, 2142.

_____ ,(1975). ibid, 8, 1686.

_____ ,(1978). ibid, 11, 7

Philibert, J. and Tixer, R. (1968). ibid, 1, 695.

Parobek, L. (1972). M. S. Thesis. The University of Western Ontario.

Rao-Sahib, T and Wittry, D. M. (1974). J. Appl. Phys., 45, 5060.

Reed, S. J. B. (1965). Brit. J. Appl. Phys., 16, 913.

Reuter, W., Kuptsis, J, D., Lurio, A. and Kyser, D. M. (1978). J. Phys. D: Appl. Phys., 11, 2633.

Sugitani, Y. (1977), Bull. Chem. Soc. Jpn., 50, 755.

White, E. W. and Jhonson, G. G. (1972). "X-ray Emission and Absorption Wavelength and Two-theta Tables", A. S. T. M. Data Series DS 37A, Philadelphia: American Society for Testing Materials.

Wittry, D. B. (1957). J. Appl. Phys., 28,58.